A STUDY ON THE DURABILITY OF FLEXIBLE PAVEMENT MATERIALS:

ASPHALT ABSORPTION AND OXIDATION KINETICS

A Dissertation

by

GUANLAN LIU

Submitted to the Office of Graduate and Professional Studies of
Texas A&M University
in partial fulfillment of the requirements for the degree of

DOCTOR OF PHILOSOPHY

Chair of Committee,	Charles J. Glover
Committee Members,	Robert L. Lytton
	James C. Holste
	Mark T. Holtzapple
Head of Department,	M. Nazmul Karim

August 2015

Major Subject: Chemical Engineering

ABSTRACT

Asphalt pavement is the major pavement type worldwide. Today, over 90% highways are paved with asphalt concrete. Like other pavement types, asphalt pavement suffers from certain types of damage, which call for maintenance. Billions of dollars are spent on the maintenance of asphalt pavement each year.

To reduce the maintenance cost, satisfactory pavement design that addresses the mechanical and chemical properties of asphalt pavement, is necessary. In pavement design, two of the factors affecting pavement durability are the absorption of asphalt into porous aggregates and the hardening of asphalt due to oxidation. Asphalt absorption reduces the effective binder content in the pavement. Meanwhile, the oxidative hardening of asphalt will eventually lead to pavement fatigue cracking.

This work focused on the properties of flexible pavement materials, especially asphalt absorption process and oxidation kinetics. The objectives were to evaluate and improve the current method of absorption measurement, and to study the oxidation kinetics of warm mix asphalt (a new pavement technology widely used). To achieve these objectives, studies were designed and conducted.

Asphalt absorption in porous materials was systematically studied. A new method for asphalt absorption measurement, using a density gradient column, was developed to measure asphalt absorption in single aggregate particles at a higher precision level. Experimental results showed that asphalt absorption correlated very well with the void volume in asphalt, regardless of the aggregate type. Moreover, the effect of

contact time on asphalt absorption was studied. Finally, the asphalt absorption of warm mix materials from loose mix samples was measured using a density gradient column.

Additionally, the oxidation kinetics of warm mix asphalt was investigated. Oxidation kinetics parameters were estimated and used in a pavement aging simulation. Insignificant differences between the warm mix asphalts and the base binder control were found. These oxidation kinetics results provided a better understanding of the pavement performance of warm mix asphalt.

DEDICATION

I would like to dedicate all of my Ph.D. work and this dissertation to my wife, as well as my parents for their love, encouragement, and support.

ACKNOWLEDGEMENTS

I am indebted to and wish to thank my committee chair, Dr. Charles J. Glover, and my committee members, Dr. Robert L. Lytton, Dr. Mark Holzapple, Dr. James Holste, for their guidance, patience, encouragement and support throughout this research.

Also, I would like to thank my colleagues, Rongbin Han, Xin Jin, Yuanchen Cui and Avery Rose. Their collaborations are indispensable for the success of my research.

Finally, thanks to my parents for their encouragement and to my wife for her love, patience and support.

NOMENCLATURE

AASHTO	American Association of State Highway and Transportation Officials
AMRL	AASHTO Materials Reference Laboratory
ASTM	American Society for Testing and Materials
ATR	Attenuated Total Reflectance
BISG	Impregnated Specific Gravity
CA	Carbonyl Area
CKE	Centrifuge Kerosene Equivalent
DGC	Density Gradient Column
DSR	Dynamic Shear Rheometer
FTIR	Fourier Transform Infrared Spectroscopy
HMA	Hot Mix Asphalt
HS	Hardening Susceptibility
LMT	Lithium Metatungstate
PAV	Pressure Aging Vessel
POV	Pressure Oxygen Vessel
RTFOT	Rolling Thin Film Oven Test
SSD	Saturated Surface Dry
TEG	Triethlene glycol
TxDOT	Texas Department of Transportation

WMA	Warm Mix Asphalt
VMA	Voids in the Mineral Aggregate
VFA	Voids Filled with Asphalt
fcf	Field Calibration Factor

TABLE OF CONTENTS

Page

LIST OF FIGURES

Page

LIST OF TABLES

Page

CHAPTER I

INTRODUCTION AND LITERATURE REVIEW

Since its first use as pavement in the 1920s, asphalt concrete has become the most common type of paved road or highway. Asphalt pavement provides improved cost efficiency, reduced noise, enhanced safety, comfort, and recyclability. Thus, it dominates over 94% of the paved road surfaces in the United States (i.e. around 2 million miles), facilitating both commercial and residential transportation. However, despite its benefits, asphalt pavement also faces multiple types of stress. Mechanical or chemical stress (such as traffic loading, moisture damage, and oxidative aging) can eventually lead to pavement cracking. Thus, a better understanding of asphalt performance and improvement of pavement durability is necessary. In response to this demand, pavement engineers have been working to improve pavement performance for decades. This research is economically promising, because the annual construction and maintenance cost of asphalt pavement exceeds billions of dollars [1]. Satisfactory pavement design is both economically and mechanically necessary to minimize potential maintenance costs while providing sufficient durability under high traffic loads.

Recently, a significant improvement of asphalt pavement technology, warm mix asphalt (WMA), has been widely used. WMA technology promises the economic benefits of reduced fuel consumption and an extended paving season plus the technical convenience of enhanced compaction and increased haul distances, because of significantly reduced mixing and compacting temperatures. Although many studies have

been done on warm mix asphalt [2-6], asphalt absorption and oxidation kinetics have not been comprehensively studied.

Asphalt absorption and oxidation kinetics both affect pavement durability. Asphalt absorption will reduce the effective binder content in the pavement whereas oxidative hardening of asphalt will eventually lead to pavement fatigue cracking. A better understanding of these two properties in asphalt pavements can help minimize the maintenance cost of pavement and improve its performance. To reach a successful WMA pavement design, it is critical to measure asphalt absorption precisely. Furthermore, to predict the pavement durability of warm mix asphalt, oxidation kinetics need to be estimated.

Objectives

To reduce the construction and maintenance cost of modern asphalt pavement technologies, this research aims to improve pavement design and durability prediction. Multiple asphalt types were selected, covering the increasingly used warm mix asphalt. Among the characteristics of asphalt pavements, this research focuses on the asphalt absorption and oxidation kinetics. The objectives follow:

First, investigate and improve the asphalt absorption measurement to provide better data for pavement design. Second, study the oxidation kinetics of warm mix asphalt and predict its potential oxidation failure.

Literature review

Warm mix asphalt

In recent years, warm mix asphalt (WMA) technologies, with significantly reduced mixing and compacting temperature, have been attracting increased attention. Deploying WMA technology in the asphalt industry promises economic benefits (reduced fuel consumption and extended paving season) plus technical convenience (enhanced compaction and increased haul distances). Popular warm mix additives include emulsion-based additives, chemical additives, and synthetic additives. To understand the effects of WMA technology on pavement performance, much effort has been invested to understand the performance of WMA pavements. In particular, warm mix asphalt oxidative aging results in pavement fatigue failure and is now recognized as an important factor in pavement design. It has been shown that some warm mix asphalt binders can change the rheological behavior after long-term aging. The driving force of these rheological changes is the chemical reaction of asphalt and oxygen, *i.e.*, asphalt oxidative aging. Thus, quantitatively understanding oxidative aging and consequent hardening is key to predicting changes in rheological behavior. However, because previous studies of warm mix asphalt focused on the mechanical properties and had limited aging states (one short-term aging state and one long-term aging state), detailed research on oxidative kinetics is not found.

Pavement mixture properties

When a sample of pavement mixture is prepared in the laboratory, it is analyzed to determine the probable performance in a pavement structure. The analysis focuses on

five volumetric characteristics and the influence those characteristics are likely to have on mixture behavior. The five characteristics are:

1) Mixture density

2) Air voids

3) Voids in the mineral aggregate (VMA)

4) Voids filled with asphalt (VFA)

5) Binder content

Mixture properties are most affected by volume rather than weight; however, production and testing of hot mix or warm mix are by weight. Example volumetric properties that determine long-term pavement performance of mixture are air voids, voids in mineral aggregate (VMA), and voids filled with asphalt (VFA).

Standard methods are available for measuring of mix properties [7, 8]. However, the specific gravity (numerically equal to density) of mixture is not directly measured in the standard method because of the difficulty of operation. As a substitute, the saturated surface dry (SSD) method was introduced according to the standard method, to estimate the volume of the mixture indirectly by assuming all of the pores are perfectly filled by water. The concept of SSD condition is shown in (Figure 1). SSD condition is established based on the operator's subjective judgement and thus introduce nonnegligible measurement error.

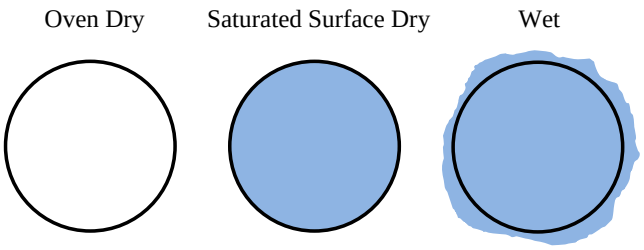

Figure 1. Saturated surface dry (SSD) condition.

Asphalt absorption

In pavement, asphalt is absorbed by the porous aggregates. Figure 2 illustrates a typical asphalt absorption status. Asphalt absorption needs to be correctly estimated for a successful pavement mixture design because it affects the effective binder content. Precise measurement of asphalt absorption in pavement is very challenging, because of the low amount of absorption. In asphalt pavement, typically the weight of aggregate is about 95 %, whereas the binder content is around 5 %. To measure absorption, people must subtract two large numbers (aggregate mass with asphalt and aggregate mass without asphalt). Even more challenging, these two large numbers are usually measured indirectly (typically by subjective SSD method).

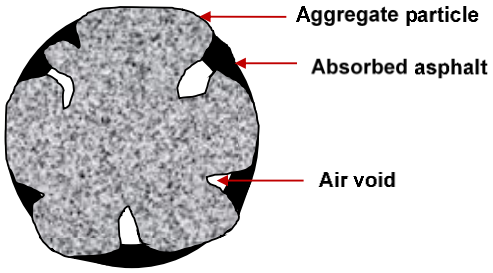

Figure 2. Asphalt absorption into porous aggregates.

Although it is challenging, because of its importance, much effort has been invested in the asphalt absorption research during the past decades. During 1940s, the Centrifuge Kerosene Equivalent (CKE) Method and the Immerse Method and Bulk Impregnated Specific Gravity (BISG) Method were developed respectively, making the asphalt absorption test possible [9, 10]. In 1969, the first comprehensive evaluations of the absorption methods (Immersion, BISG and Rice) was done by Lee [11]. In Lee's research, the physical and chemical properties of eight aggregate types and six asphalt binders with different penetration levels were measured and investigated. Asphalt absorptions were measured using all of the three method described above. It was found that the asphalt properties, the method chosen and the contact time affect asphalt absorption. Nevertheless, a high degree of absorption variability is found among aggregate particles, regardless of the aggregate type. Thus, the porosity and pore-size distribution of aggregate are believed to significantly affect asphalt absorption. Meanwhile, asphalt absorption was found to highly correlate with water absorption.

The effect of pore size distribution was further studied by Kandhal and Lee [12, 13]. These studies suggest that a pore diameter of 0.05 μm was the threshold size below which no apparent asphalt absorption occurred. Also, the effects of contact time on asphalt absorption were studied and correlated to the aggregate/asphalt properties [14, 15].

Asphalt oxidation

Asphalt oxidation and subsequent hardening have been well recognized as major causes of pavement failure. It has been widely reported that pavement durability is

highly related to binder stiffness [16-20]. A critical value (2 - 3 cm) of 15 ℃ ductility at 1 cm/min was suggested to correspond to pavement cracking [19]. Asphalt oxidation can significantly increase pavement stiffness. There are strong evidences that asphalt oxidation happens in the whole depth of pavement, dramatically affecting pavement durability [21, 22].

A series of work has been conducted to study oxidation kinetics of asphalt [22-24]. One key finding is that carbonyl growth correlates with the oxygen consumption linearly, promising carbonyl area (CA, defined as the peak area above the 1820 cm^{-1} baseline and from 1820 to 1650 cm^{-1}) value to be a reliable indicator of asphalt oxidation [23]. The constant-rate-period carbonyl formation can be expressed as the following equation:

$$r = AP^{\propto}e^{-\frac{E_a}{RT}} \quad (1)$$

where A is the frequency factor, P is the oxygen partial pressure, α is the reaction order, E_a is the constant-rate activation energy, R is the ideal gas constant, and T is the temperature (K).

Recently, Jin proposed a new model to describe oxidation kinetics [25], addressing both the constant-rate period and the fast-rate period. This model assumes that carbonyl formation follows two parallel reaction. This model fit multiple asphalt binders well. The expression of this fast-rate-constant-rate reaction model is

$$CA = CA_{tank} + M\left(1 - e^{-k_f t}\right) + k_c t \quad (2)$$

$$k_f = A_f e^{-\frac{E_{af}}{RT}} \quad (3)$$

$$k_c = A_c e^{-\frac{E_{ac}}{RT}} \quad (4)$$

where *CA* is the carbonyl area of asphalt sample, CA_{tank} is the carbonyl area of unaged asphalt, $M=CA_0 - CA_{tank}$ (CA_0 is the zero-time intercept of the constant rate reaction), k_f is the fast-rate reaction constant, k_c is the constant-rate reaction constant, A_f and A_c are pre-exponential factors for k_c and k_f, E_{af} and E_{ac} are the apparent activation energies for k_c and k_f, and R is the idea gas constant (8.314 J/mol/K).

With the kinetics parameters estimated, a pavement oxidation model was also developed to predict the pavement aging of asphalt. The governing equation of this model is shown below:

$$\frac{\partial P(x,t)}{\partial t} = \frac{\partial y}{\partial x}\left(fcf \cdot D_0 \frac{\partial P}{\partial x}\right) - \frac{c}{h} \cdot \frac{\partial CA(x,t)}{\partial t} \quad (5)$$

Principle concepts of this model are briefly explained. *P* means the partial pressure of oxygen in the asphalt, *t* refers to time, *x* means the distance to air void/asphalt interface, *c* is the factor convert *CA* formation rate to oxygen consumption rate, *h* is the solubility constant of oxygen in asphalt. A field calibration factor (*fcf*) is introduced to adjust D_0. The initial condition of this model is zero oxygen concentration in asphalt; the boundary conditions are partial pressure equals 0.2 (atm) at the air void/asphalt interface and $\frac{\partial P(x,t)}{\partial x}\Big|_{x=D_d} = 0$.

Dissertation outline

This dissertation is organized as follows: Chapter II introduces the application of density gradient column to the pavement materials addressing the aggregate

characteristics and asphalt absorption. Chapter III further explores the asphalt absorption at different contacting conditions, as well the asphalt absorption in loose-mix samples. Chapter IV studied the oxidation kinetics of warm mix asphalt. Chapter V summarized the dissertation and provided the recommendations for future work.

CHAPTER II

APPLICATION OF DENSITY GRADIENT COLUMN TO FLEXIBLE PAVEMENT MATERIALS: AGGREGATE CHARACTERISTICS AND ASPHALT ABSORPTION[*]

Accurate measurements of aggregate volumetric properties are essential to a satisfactory mix design and successful production of pavement. Moreover, determination of asphalt absorption in aggregates is required to correctly estimate air voids and adjust binder content. However, the conventional method suffers from precision issues, as well as veiling the variations among individual aggregate pieces. The object of this research is to apply the density gradient column technique to flexible pavement materials, investigating the aggregate volumetric properties, asphalt absorption, and their potential correlation. Experimental results indicated that the density gradient column could effectively measure volumetric properties and asphalt absorption of individual aggregate pieces. Furthermore, data analysis demonstrated that asphalt absorption correlates very well with void volume.

Introduction

Accurate measurements of aggregate volumetric properties and absorption are essential to develop of satisfactory mix design and production [26]. The key to

[*] Parts of this chapter are reprinted with permission from "Application of density gradient column to flexible pavement materials: Aggregate characteristics and asphalt absorption" by Guanlan Liu, Xin Jin, Avery Rose, Yuanchen Cui and Charles J. Glover. 2014. *Construction and Building Materials,* Vol. 72, 182-188, Copyright 2014 by Elsevier.

calculations of volumetric properties are aggregate specific gravities, which are numerically equal to densities (assuming density of water to be 1.0 g/cm^3). Aggregate bulk density and apparent density allow conversion between mass and volume, thus providing a reliable way to predict other necessary volumetric properties such as air void percent, void filled by asphalt (VFA), voids in the mineral aggregate (VMA), and asphalt absorption [27]. Therefore, precise and reliable measurements of aggregate densities are fundamental to the quality of hot mix asphalt or warm mix asphalt pavements.

For several decades, various laboratory tests have been used to evaluate asphalt absorption at different conditions, which is necessary for successful mix designs [11, 12, 28-30]. In paving mixtures, asphalt is absorbed by the porous structure of aggregates. Asphalt absorption is important because incorrect estimates translate into erroneous calculations of air void percent, VFA and VMA, all important parameters used in mixture design to control pavement durability and stability. It has been reported that asphalt absorption is a process controlled by capillary force that depends both on asphalt properties (including asphalt composition, viscosity, and surface tension) and aggregate properties (such as porosity, pore size distribution and surface chemical composition) [13, 31]. Particularly, comparison of water absorption and asphalt absorption shows they are correlated [11]. The driving force for asphalt absorption is mainly determined by capillary action and absorption is reported to be a nonlinear function of time [13]. It also has been reported that aggregate tends to selectively absorb some asphalt components

over others [32]. Recent studies of aggregate volumetric properties and asphalt absorption in asphalt pavement can also be found [33-37].

Although standard testing procedures are available to measure volumetric properties and asphalt absorption in aggregates [7, 8, 38], these standard methods have some limitations [39]. The first problem is precision. Measuring aggregate volumetric properties requires achieving a saturated surface dry (SSD) condition of the aggregate, a rather subjective assessment and therefore difficult to reproduce precisely or accurately among investigators. Also, precision is limited by the inherent difficulty of measuring volume accurately and subtracting two large numbers that differ by a small amount. Second, standard methods are inadequate to understand the fundamentals of asphalt absorption. The standard methods are based on measurements of samples comprised of large numbers of aggregate pieces having variable properties. However, asphalt absorption varies according to the properties of each specific aggregate piece. Reporting average results on large samples veils individual differences between aggregate pieces.

The density gradient column (DGC), often used for determining the densities of small samples of polymers and other materials, is based on the preparation of a stable column of single-phase liquid of variable density along its length [40-42]. A specimen introduced into the column is supposed to settle at a level of known density (determined by using precisely manufactured and calibrated beads of known density), where it is in hydrostatic equilibrium with the fluid in the column. In DGC, the density of small specimens can be measured quite precisely. A key feature that improves precision is that density is measured directly rather than mass and volume separately. Although DGC has

been used for polymer and other materials test, it has not been applied to aggregate densities and absorption measurements.

Objective

A principal objective of this study was to adapt the DGC method to flexible pavement materials to more accurately measure aggregate bulk and apparent densities and water and asphalt absorption. Part of achieving improved precision was to eliminate the subjective saturated surface dry (SSD) measurement. In addition, this approach provides a method of measuring aggregate bulk and apparent densities and the ability to compare asphalt absorption directly to water absorption, i.e., to the aggregate void volume. An additional objective was to compare the precision of the DGC method for asphalt absorption to the precision of using the standard methods and practice for measuring asphalt absorption.

Materials & methods

Materials

Six types of pavement coarse aggregates (Delta Sandstone, Martin Marietta Granite, TX1 Lightweight Streetman, Jones Mill Quartzite, Hanson Limestone, Hoban Rhyolite Grade 6 Gravel) and one asphalt binder (Alon PG 64-22) were selected for the study. To generate a liquid density gradient suitable for pavement aggregate materials, lithium metatungstate (LMT) heavy liquid and glass calibration beads were obtained. Paraffin wax was used as a coating to determine aggregate bulk density.

Density gradient column development

The density gradient method is based on the direct measurement of particle density in a column of fluid that has a linear density gradient. The gradient is generated by continuously blending two completely miscible make-up fluids of different densities and feeding them slowly to the bottom of the column. For asphalt binder measurements the two make-up fluids are water and a brine solution of appropriate density. For aggregate measurements, the two make-up fluids are water and a heavy liquid (lithium metatungstate, density 2.95 g/cm^3). The heavy liquid is regenerated by evaporating the water.

The DGC method is direct and efficient because it does not require measuring particle volume, a difficult measurement to do precisely. Instead, the accuracy of DGC method depends upon an accurate calibration of the density variation with position in the column. Two sets of glass beads (American Density Materials, Inc., 3826 Spring Hill Road, Staunton, VA 24401-6318), traceable to NIST weights and measures, were used for calibrations; one set (for asphalt density determinations) provides density calibrations at 23℃ from 0.94 to 1.10 g/cm^3 +/- 0.0002 g/cm^3 and the other set (for aggregate density determinations) provides density calibrations from 2.0 to 2.8 g/cm^3 +/- 0.0005 g/cm^3. The thermal expansion of the beads was provided as 0.000037 $g/(cm^3 \cdot ℃)$. An example calibration of a column prepared for aggregate measurements is presented in the Results and Discussion section. The measurement requires generating a linear density fluid in an appropriate graduate cylinder containing the calibration beads. The beads, each of different density, settle at the point in the column equal to their density. Particles of

asphalt or aggregate are dropped into a column of appropriate density range and settle at the position corresponding to their density. The position of each bead or asphalt or aggregate particle was read with a cathetometer of 0.001 cm precision. The asphalt or aggregate densities were determined by linear interpolation of this density versus vertical position calibration.

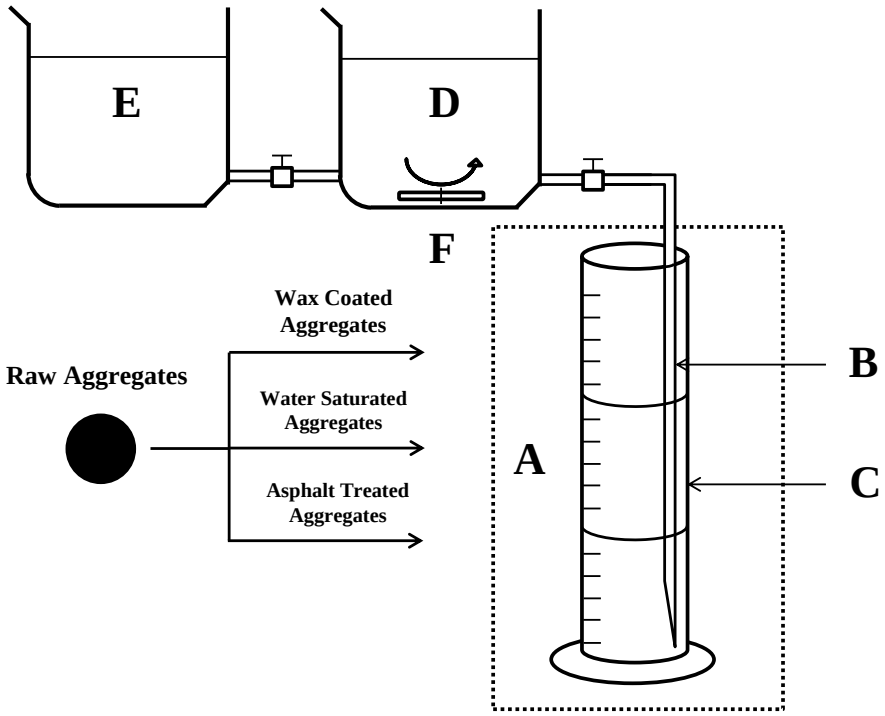

Figure 3. The schematic diagram for density gradient column.
(A: density gradient column area; B: capillary tube; C: column; D: low density liquid; E: high density liquid; F: magnetic stirring bar)

Figure 3 shows a schematic of the DGC; aggregate particles of varying states were dropped into the DGC to measure their density. These states included wax-coated, water-saturated, and asphalt-treated, which are described below.

Asphalt absorption calculation

The DGC methodology requires immersing the aggregate under melted asphalt binder at 121 ℃ for 15 s on a hot plate followed by curing the coated aggregate at 143 ℃ for 2 h in the oven, to approximate TxDOT specifications on laboratory preparation of asphalt mixture [43]. The mass of asphalt absorbed by aggregate $m_{abs\text{-}b}$ is determined by subtracting the aggregate mass from the mass of aggregate plus absorbed and coated asphalt and then correcting for the mass of asphalt coating:

$$m_{abs-b} = f(m_{ab}, m_a, \rho_b, \rho_{ab}, \rho_{av}) = m_{ab} - m_a - \frac{m_{ab}\rho_b}{\rho_{ab}} + \frac{m_a\rho_b}{\rho_{av}} \quad (6)$$

where m_{ab} is the mass of aggregate coated with asphalt (including both absorbed asphalt and excess asphalt coating), m_a is the mass of aggregate (including air voids of negligible mass), ρ_b is the asphalt density, ρ_{ab} is density of asphalt-treated aggregate (including both absorbed asphalt and excess asphalt coating), ρ_{av} is bulk density of the aggregate, i.e., the density of the aggregate including its air voids. The masses were measured using a precision balance, and densities were measured using the DGC. While the first four properties can be measured directly, ρ_{av} is measured using the wax-coating method described below.

Bulk density determination

The bulk density of a single aggregate particle is the density (mass/volume) of the aggregate including its accessible air-void volume. The bulk density of a sample of many aggregate particles is the density (mass/volume) including all of the particle accessible internal air voids but excluding the void spaces in the interstices between particles. Thus, the bulk density of an aggregate sample of many particles is an average

bulk density of those particles. In the standard method, a saturated surface dry (SSD) condition is necessary to determine aggregate bulk density. Under this SSD condition, the pores of aggregate particles are filled with water and no excess water is on the particle surfaces (i.e., in the spaces between particles). The SSD condition is experimentally achieved by removing this excess water from the aggregate by absorbing surface moisture with towels (for large aggregate) or allowing finer aggregate to dry to "the appropriate state." This method is subjective to an operator's judgment and also difficult to achieve uniformly. Thus, achieving the SSD condition is likely one of the main limits to the precision of aggregate bulk density measurements.

To achieve better precision of bulk density measurements (for single particles), a wax coating method was developed. This method is designed to coat the aggregate (paraffin wax, Avantor Performance Materials, Inc., Philipsburg, NJ 08865) without absorption into the pores. The aggregate is chilled in a refrigerator and molten wax, near its melting point is coated onto the surface of aggregate with a fine brush, taking care to fill the surface contours. In this procedure, the cold aggregate freezes the wax upon contact and prevents it from penetrating into the aggregate pores. The bulk density is calculated using the following equation, with the amount of absorption (in this case of wax) assumed equal to zero:

$$0 = m_{ac} - m_a - \frac{m_{ac}\rho_c}{\rho_{ac}} + \frac{m_a\rho_c}{\rho_{av}} \tag{7}$$

from which the aggregate bulk density ρ_{av} is calculated as:

$$\rho_{av} = \frac{m_a\rho_c}{m_a + m_{ac}\frac{\rho_c}{\rho_{ac}} - m_{ac}} \tag{8}$$

where m_{ac} is the mass of the wax-coated aggregate, m_a is the mass of the uncoated aggregate, ρ_c is the density of wax, and ρ_{ac} is the density of the wax-coated aggregate.

Apparent density measurement

The aggregate apparent density is the aggregate mass per volume excluding the accessible air-void volume (but including trapped void volume inside the aggregate particles). Vacuum water saturation for 45 min, followed by 24-h additional water immersion are applied before measuring the density of the water-saturated aggregate in the DGC. The apparent density of the aggregate is calculated using the flowing equation:

$$\rho_a = \frac{1}{\frac{1}{\rho_{av}} - \frac{1}{\rho_w}\left(\frac{\rho_{aw}}{\rho_{av}} - 1\right)} \tag{9}$$

where ρ_a and ρ_{av} are as defined above, ρ_{aw} is the density of water-saturated aggregate and ρ_w is the density of water at the laboratory temperature.

Accessible void volume calculation

With the aggregate mass and densities determined, the (accessible) void volume (V_{void}) of each aggregate was calculated as its bulk volume minus the aggregate apparent volume:

$$V_{void} = \frac{m_a}{\rho_{av}} - \frac{m_a}{\rho_a} \tag{10}$$

Results and discussion

Statistical analysis of standard practice

The conventional practice for asphalt absorption calculation is ASTM D4469, which suffers from precision issues. Using typical measurement values for each variable and reported ASTM reproducibility precision limits for each variable in the method's

calculation, the method reports that because of random measurement errors, an example calculated value of asphalt absorption may range from -0.38 to +3.05% (of dry aggregate weight)! Although this method is for pavement mixtures and the errors can be better controlled in the laboratory, the same fundamental difficulties exist for measurements on laboratory specimens. Table 1 shows the example of measurement error in the standard method.

Table 1. Effect of measurement errors on calculated percent asphalt absorption in ASTM D4469 (adapted from Table X1.1, ASTM D4469, 2011).

Theoretical Maximum Specific Gravity	Asphalt Content %*	Asphalt Apparent Specific Gravity	Weighted Average ASTM Oven-Dry Bulk Specific Gravity of Total Aggregate	% Asphalt Absorption
2.501	6.2	1.015	2.673	1.32
2.482(a)	6.2	1.015	2.673	0.98
2.520(a)	6.2	1.015	2.673	1.64
2.501	5.39(a)	1.015	2.673	0.77
2.501	7.01(a)	1.015	2.673	1.87
2.501	6.2	1.013(a)	2.673	1.33
2.501	6.2	1.017(a)	2.673	1.31
2.501	6.2	1.015	2.615(a)	2.16
2.501	6.2	1.015	2.731(a)	0.51

*Asphalt content based on mass of sample of total oven dry mix (kg of asphalt per 100 kg of oven dry total mix)

Error propagation was also done on the conventional method, calculation result indicate that if the volumetric properties error are as required by ASTM standards, the asphalt absorption error calculated could be up to 98 % (the Difference Two-Sigma

Limit in percent) for multiple laboratory measurements [44]. This precision level is not sufficient to distinguish asphalt absorption at different conditions. Details of this error propagation are provided in the appendix.

DGC calibration

Figure 4 shows example DGC linear calibration, with a range designed for aggregate density measurements. The density of the aggregate is determined by measuring each aggregate's vertical position in the column using the telescopic cathetometer having a precision of 0.001 cm. Additionally, the paraffin wax density (0.917 g/cm^3) and the Alon PG 64-22 asphalt density (1.036 g/cm^3) were measured. The two column fluids used to create the DGC for measuring the wax density were water and isopropyl alcohol, a very poor solvent for the wax.

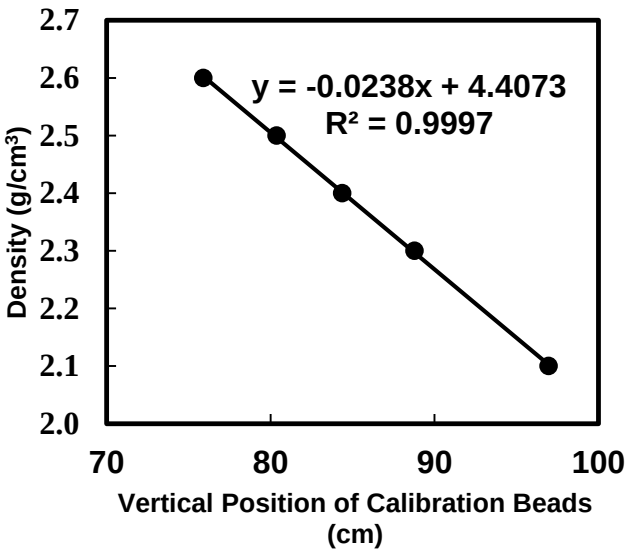

Figure 4. Example DGC density versus vertical position calibration.

Aggregate characteristics

From DGC measurements, piece-by-piece aggregate mass, bulk density, apparent density, void volume, and void fraction were measured for five natural aggregate materials and one lightweight, manufactured material. Data for Hanson Limestone and Jones Mill Quartzite are shown in Table 2 and Table 3.

Table 2. Aggregate characteristics, Hanson Limestone (n = 10)

Aggregate	**Mass (g)**	**Bulk Density (g/cm^3)**	**Apparent Density (g/cm^3)**	**Void Volume (cm^3)**	**Void Fraction**
Hanson Limestone	0.9145	2.491	2.798	0.040	11%
Hanson Limestone	0.9289	2.560	2.787	0.029	8%
Hanson Limestone	0.5146	2.510	2.739	0.017	8%
Hanson Limestone	1.2332	2.635	2.718	0.014	3%
Hanson Limestone	0.4096	2.624	2.712	0.005	3%
Hanson Limestone	0.4866	2.587	2.673	0.006	3%
Hanson Limestone	0.7165	2.513	2.903	0.038	13%
Hanson Limestone	0.5355	2.612	2.697	0.006	3%
Hanson Limestone	0.8588	2.597	2.753	0.019	6%
Hanson Limestone	1.0510	2.645	2.688	0.006	1.6%

Table 3. Aggregate characteristics, Jones Mill Quartzite (n = 7)

Aggregate	Mass (g)	Bulk Density (g/cm^3)	Apparent Density (g/cm^3)	Void Volume (cm^3)	Void Fraction
Jones Mill Quartzite	0.5587	2.369	2.802	0.036	15%
Jones Mill Quartzite	0.2840	2.536	2.806	0.011	10%
Jones Mill Quartzite	0.3256	2.492	3.041	0.024	18%
Jones Mill Quartzite	0.6626	2.412	3.098	0.061	22%
Jones Mill Quartzite	0.2766	2.550	2.908	0.013	12%
Jones Mill Quartzite	0.2705	2.579	2.831	0.009	9%
Jones Mill Quartzite	0.3184	2.519	2.888	0.016	13%

Table 4 reports The data for all six aggregate types (Delta Sandstone, Martin Marietta Granite, Hanson Limestone, Hoban rhyolite grade 6 Gravel, Jones Mill Quartzite, and TX1 Lightweight Streetman), including statistical measures. It is clear that even for the same type and source of aggregate, intrinsic aggregate properties show significant differences between individual pieces; for example, air void fractions are not distributed evenly among the separate aggregate pieces. Also notable is the variation in average void fraction among the six aggregates, ranging from 0.06 for Hanson Limestone to 0.33 for manufactured lightweight material.

Table 4. Average characteristics for samples of six aggregate types

Aggregate		Mass (g)	Bulk Density (g/cm^3)	Apparent Density (g/cm^3)	Void Volume (cm^3)	Void Fraction (%)
Delta Sandstone	AVG	0.9773	2.346	3.062	0.101	23
(***n*** **= 9)**	SD	0.3807	0.192	0.147	0.080	9
Granite	AVG	0.5016	2.504	2.850	0.024	12
(***n*** **= 7)**	SD	0.1643	0.060	0.121	0.011	5
Hanson Limestone	AVG	0.7649	2.577	2.747	0.018	6
(***n*** **= 10)**	SD	0.2863	0.050	0.070	0.012	4
Gravel	AVG	0.5756	2.399	2.835	0.038	15
(***n*** **= 14)**	SD	0.2157	0.060	0.127	0.021	5
Jones Mill Quartzite	AVG	0.3852	2.494	2.911	0.024	14
(***n*** **= 7)**	SD	0.1583	0.076	0.117	0.019	5
Lightweight	AVG	0.3167	1.504	2.269	0.069	33
(***n*** **= 7)**	SD	0.1713	0.044	0.166	0.043	6

Note: AVG: average; SD: standard deviation

It should be noted that the measurement uncertainty is much less than the piece-to-piece variability, which is dominated by inherent aggregate properties. Based on the aggregate calibration bead uncertainty of 0.0005 g/cm^3, a void fraction uncertainty (estimated by error propagation and expressed as a fraction of the aggregate accessible voids) is estimated to range from 0.001 (for the Delta Sandstone) to 0.004 (for the Hanson Limestone). It is expected that the actual density uncertainty would be greater than for the calibration beads; thus, if the uncertainty is a factor of 10 greater (i.e., ± 0.005 g/cm^3), similar to the ASTM reported precision, then these uncertainty ranges would be from 0.01 to 0.04 respectively, i.e., from 1 % to 4 % of these calculated void volumes. These values would translate directly to water absorption uncertainty and

compare to ASTM fine and coarse aggregate precision ranges of from approximately three to 20 % of the average value [7, 8, 38].

Asphalt absorption

Table 2, Table 3 and Table 4 show the DGC method can be used to measure asphalt absorption on an aggregate piece-by-piece basis, thus providing the ability to relate absorption directly to the other aggregate characteristics. Typically, asphalt absorption is expressed per mass of aggregate, suggesting that for a given type of aggregate, absorption is proportional to mass. However, data in Figure 5 show that this presumption is not necessarily true. There may be a linear correlation on a per mass basis, as for the Jones Mill quartzite aggregate, or there may be no correlation, as for the Hanson Limestone.

Factors important to asphalt absorption

To evaluate factors important to asphalt absorption, several aggregate properties provided by DGC measurements were evaluated. Figure 6 shows the relationship of void volume to aggregate mass for individual pieces of Hanson Limestone and Jones Mill quartzite. For the Hanson Limestone, there is no correlation whereas for the Jones Mill quartzite, the void volume follows a clear linear correlation with aggregate mass. These two different relations are consistent with those shown in Figure 5 and suggest that the volume of absorbed asphalt relates to the aggregate void volume, relationships that are shown in Figure 7. The origin for each data set is not considered an *a priori* data point in these plots, but certainly, it is very consistent with the results. It is clear that there are very good linear relationships between asphalt absorption volume and void volume.

Apparently, void volume is a more meaningful property for describing and correlating asphalt absorption than aggregate mass.

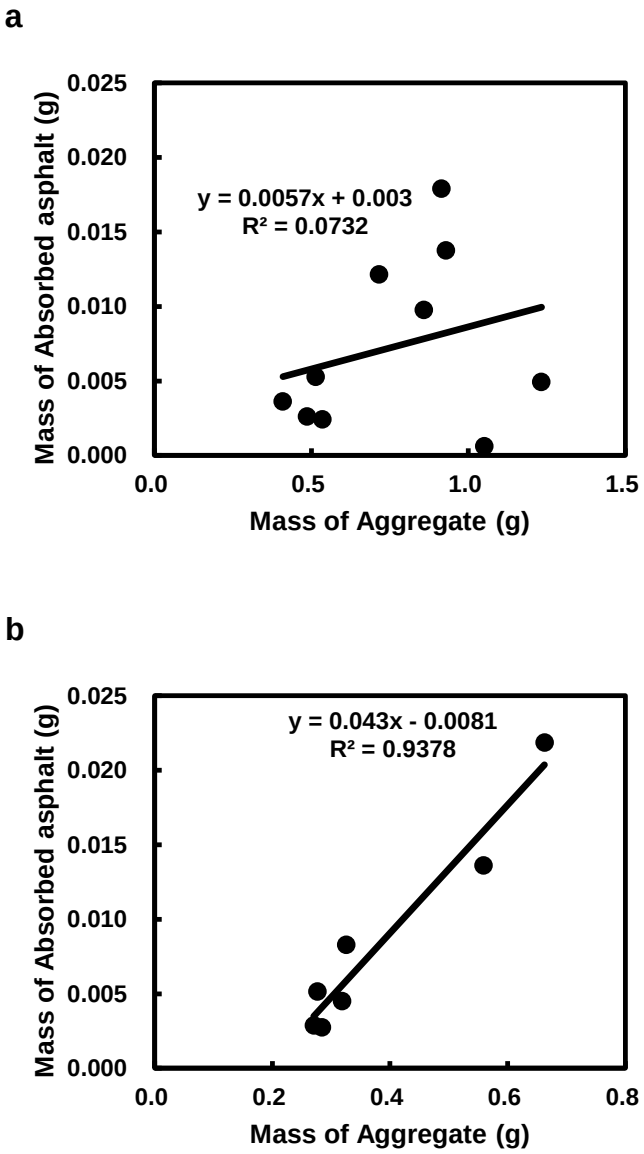

Figure 5. Relationship of asphalt absorption versus mass of aggregate, (a) Hanson Limestone, (b) Jones Mill Quartzite.

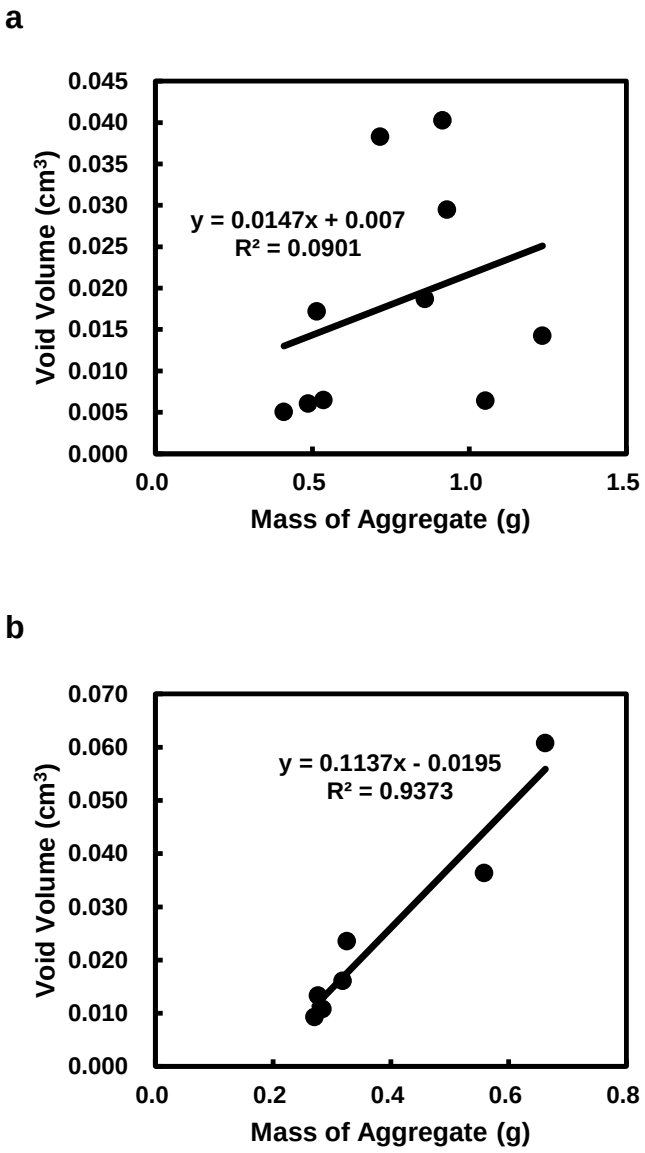

Figure 6. Air voids distribution in individual aggregate pieces, (a) Hanson Limestone, (b) Jones Mill Quartzite.

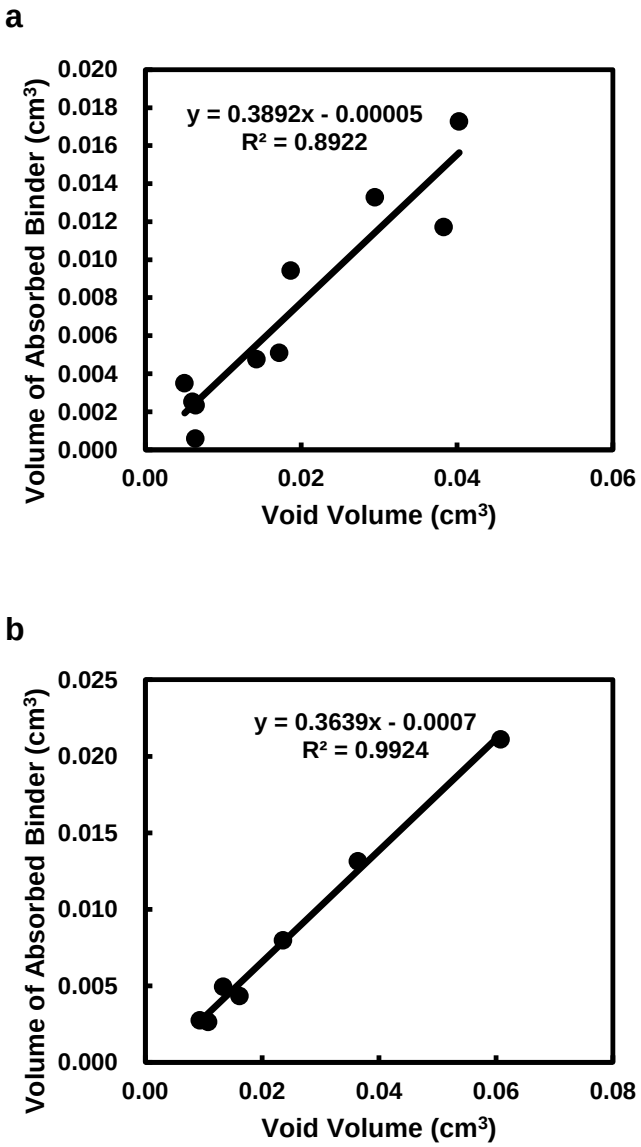

Figure 7. Relationship of air voids volume and volume of absorbed asphalt, (a) Hanson Limestone, (b) Jones Mill Quartzite.

Importance of void volume to asphalt absorption

To verify the importance of void volume in absorption research, DGC absorption data were obtained for additional types of aggregate. Delta Sandstone, Granite, Gravel, and Lightweight aggregate also were evaluated. All of these experiments used Alon 64-22 asphalt binder with 15 s mixing (immersion) time at 143 ℃ followed by 2 h curing time at 121 ^{0}C. Figure 8 shows absorbed asphalt volume versus aggregate void volume for all six types of aggregates. Again, the piece-by-piece aggregate asphalt absorption correlates very well with the aggregate air voids. Moreover, this type of correlation is found for all six types of aggregates (Delta Sandstone, Martin Marietta Granite, Hanson Limestone, Jones Mill quartzite, gravel, and lightweight manufactured aggregate), indicating that the aggregate void volume plays a key role in determining asphalt absorption. As noted below, with the exception of manufactured lightweight aggregate, the slopes of the correlations for the five natural aggregate materials are 0.4 (to within 95% confidence intervals), indicating that for the same asphalt and identical mixing/curing condition protocol, the percentages of void volume ultimately occupied by the asphalt is similar for these five different aggregate types.

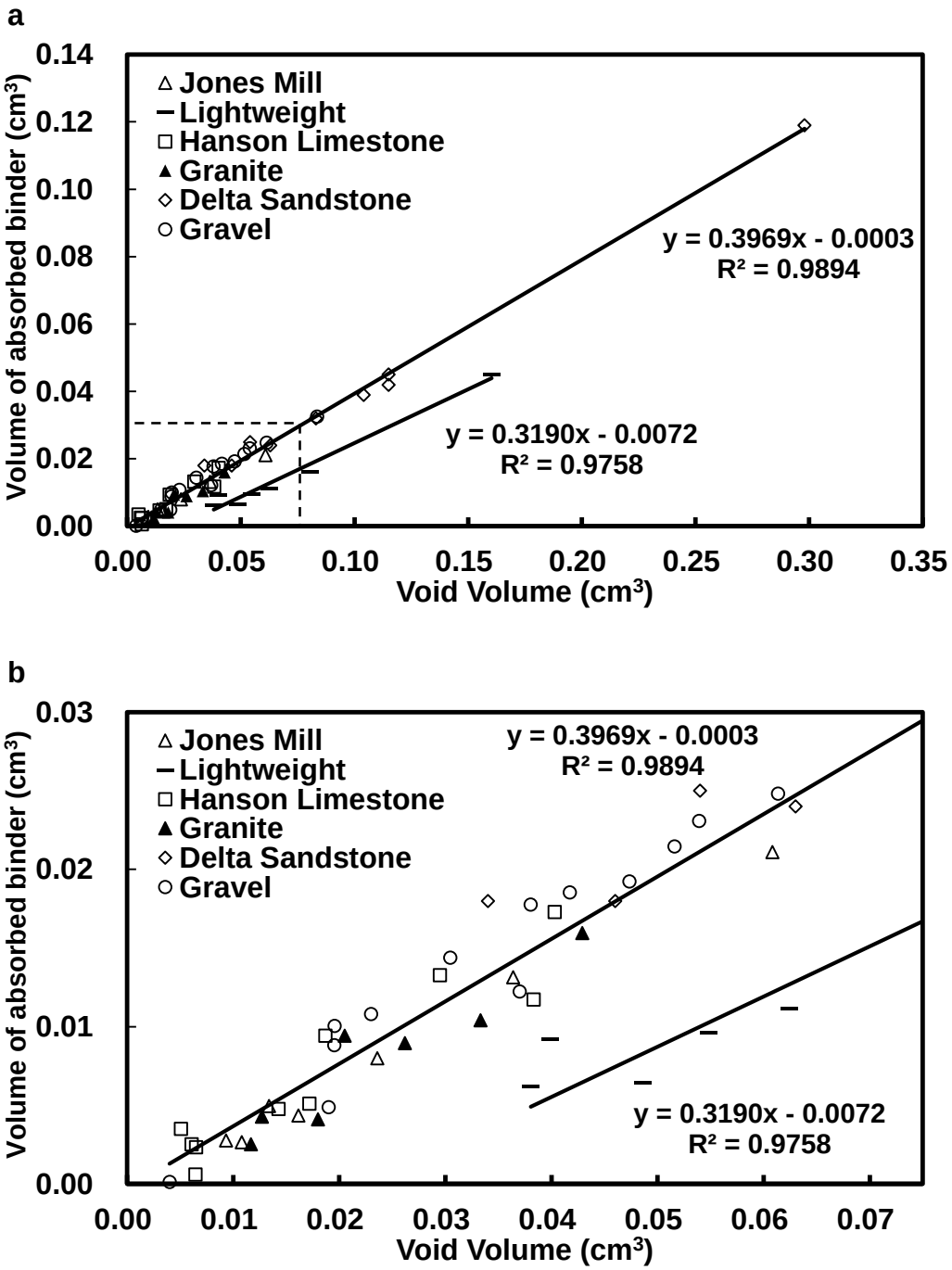

Figure 8. Correlation of void volume and volume of absorbed asphalt on (a) the six aggregate types and (b) the six aggregate types near the origin**.**

Statistical analysis

Table 5 summarizes statistical analysis on the DGC regression equations, which is compared to data of Lee [11]. Lee presented a careful and thorough study of absorption using standard absorption methods (Rice, immersion, and bulk impregnated specific gravity) on a large number of aggregate types and four binders of different penetration grade. The number of absorption determinations in each case provides a unique data set for evaluating the precision of these methods.

The DGC method provides data of greater precision than methods reported by Lee, as reflected by a greater R^2 and more precise estimates of regression coefficients (smaller standard error in both slope and intercept), for the same or smaller sample size. Also, it is notable that standard errors of the intercepts for the DGC data are dramatically less than for Lee's data.

Table 5. Regression equations and statistical analysis: asphalt absorption versus void volume

Methodology	Materials	Regression equation	R^2	*n*	SE_a	SE_b
Rice*	127-1	$Y = 0.5162X - 0.1584$	0.9137	18	0.0397	0.1947
	127-2	$Y = 0.5067X - 0.4106$	0.9059	16	0.0436	0.2264
Immersion*	127-1	$Y = 0.7760X + 0.0137$	0.8103	16	0.1003	0.4616
	127-2	$Y = 0.6749X + 0.5041$	0.8221	14	0.0906	0.4380
BISG*	127-1	$Y = 0.6604X + 0.1155$	0.8367	24	0.0622	0.2806
	127-2	$Y = 0.5822X - 0.3876$	0.7626	27	0.0650	0.2812
Density Gradient Column	Sandstone	$Y = 0.3905X + 0.0007$	0.9933	9	0.0121	0.0015
	Granite	$Y = 0.3908X - 0.0013$	0.9018	7	0.0577	0.0015
	Limestone	$Y = 0.3892X - 0.00004$	0.8922	10	0.0478	0.0011
	Gravel	$Y = 0.4030X + 0.0004$	0.9581	14	0.0243	0.0010
	Quartzite	$Y = 0.3639X - 0.0007$	0.9924	7	0.0143	0.0004
	Lightweight	$Y = 0.3190X - 0.0072$	0.9758	7	0.0225	0.0018
	Natural**	$Y = 0.3969X - 0.0003$	0.9894	47	0.0061	0.0004

Note: *Y*: dependent variable, volume of asphalt absorption; *X*: independent variable, void volume; SE_a: standard error of slope; SE_b: standard error of intercepts; *n*: points in linear regression; *literature data; **Five natural aggregate types, this study (excludes manufactured lightweight).

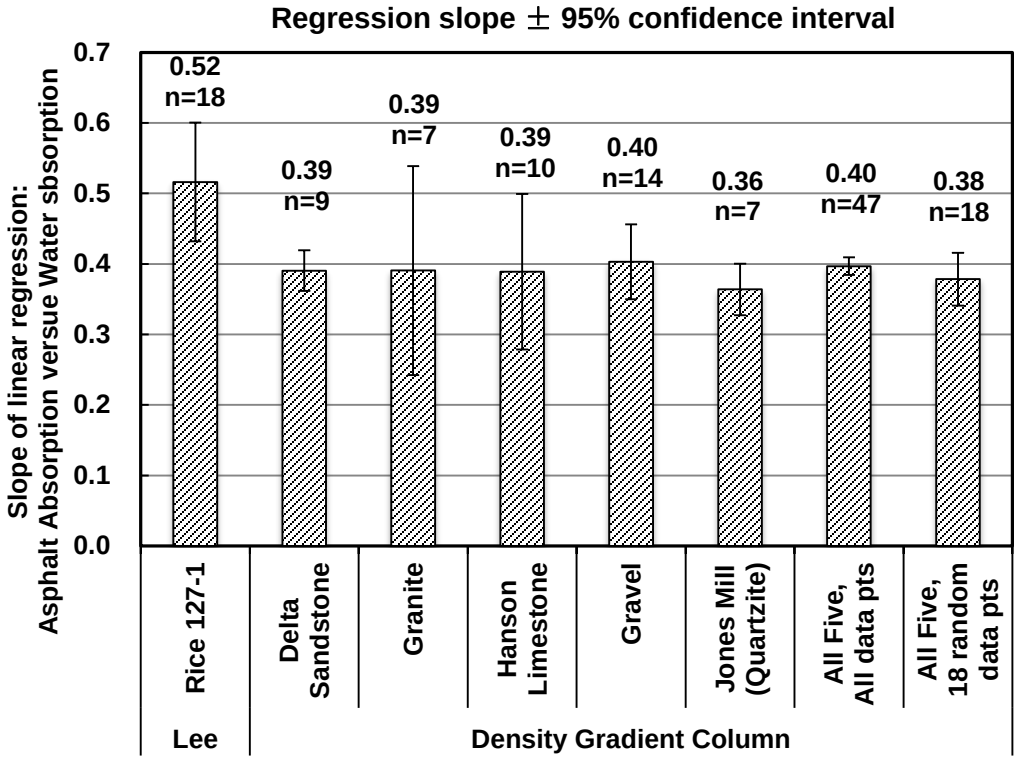

Figure 9. Summary of asphalt absorption Rice 127-1 data of Lee [11] and DGC method data.

To further quantify the regression parameter precision, 18 points from the DGC data for the five natural aggregates (47 aggregate pieces) were randomly selected to match the number of regression points reported by Lee [11] on his asphalt absorption data set, Rice 127-1. For these 18 data points, the 95% confidence intervals for the slope is 0.037 for the DGC method versus 0.084 for the Rice 127-1 data; the intercept confidence interval is 0.002 for DGC versus 0.413 for the Rice method.

Interestingly, this DGC linear correlation is strengthened considerably when statistically analyzing the regression parameters based on the 47 data points for all five natural aggregates studied (excluding the manufactured lightweight material). The 95% confidence intervals for the overall regression parameters are 0.012 for the slope and 0.001 for the intercept.

Figure 9 summarizes Rice 127-1 data and the DGC results. The difference in slopes (average absorption level) for the two methods is likely due to differences in the immersion and curing protocols. The interesting feature appears to be that a consistent protocol provides a consistent absorption level, when viewed as a function of void volume. Furthermore, although the DGC method provides more precise measurements than the standard methods and thus can be used as a tool to explore the fundamentals of aggregate absorption, it is limited to characterizing absorption on individual aggregate pieces of a single aggregate size range rather than aggregate samples large enough to represent mixture aggregate coarse or fine samples.

Conclusions

Tto better understand the fundamentals of flexible pavement materials, the density gradient column (DGC), a precise and efficient tool to measure the density of small particles, was successfully applied to this research. Characteristics of individual aggregate pieces including volumetric properties and asphalt absorption were investigated. Also, the relationship between these aggregate properties and asphalt absorption was studied. The key findings of this study follow:

- The DGC provides a convenient method for measuring aggregate bulk density and apparent density, for individual aggregate pieces. From these data, other volumetric properties of aggregate pieces such as air void fraction can be calculated. Although this procedure would require many measurements to representatively characterize an entire aggregate source, the method has the advantage of providing specific aggregate characteristics and as such, can provide an improved understanding of the importance of these fundamentals to pavement materials.
- Analysis of sets of aggregate pieces shows (unsurprisingly) that different aggregate types may possess inherently different volumetric properties. Interestingly, even for the same aggregate type, there can be significant variability among individual aggregate pieces in their void volume and void fraction. For example, the void fraction (void volume per bulk volume) for Hanson Limestone varied from 1.6 % to 13 % for a sample of 10 pieces of aggregate, with the range in average void fraction for the five natural aggregate samples studied varying from 6 % to 23 % and the manufactured lightweight aggregate material at an average void fraction of 33 %.
- The density gradient column provides the capability to determine asphalt absorption for individual aggregate pieces, thus allowing correlations between the amount of asphalt absorption and other aggregate-specific properties to be explored. Experimental results indicate that asphalt absorption generally correlates well with aggregate void volume and may not correlate at all with

aggregate mass. This conclusion holds for all six aggregate types that have been characterized in this work, indicating that a volumetric-based correlation is fundamental to aggregate absorption.

- Statistical analysis of the linear regression coefficients relating asphalt absorption to void volume show that the DGC provides significantly more precise results than the standard practice allow, with much smaller scale and less replicates (around 10 pieces of aggregates, ranging from 0.5 to 2 g each piece). Thus, the DGC method can be a valuable tool to study small number of samples at different conditions, which is vital to reveal the fundamental process of asphalt absorption.

CHAPTER III

FURTHER EXPLORATION OF ASPHALT ABSORPTION

The density gradient column method has been established as a reliable and more precise way to measure asphalt absorption. Also, evidence showed that volume of absorbed asphalt was correlated with aggregate void volume, regardless of other aggregate characteristics, providing a universal indicator of asphalt absorption. These findings promise the further utilization of density gradient column method on asphalt absorption, for multiple materials under various conditions. In this chapter, two more detailed asphalt absorption research were conducted.

First, a subsequent research on contacting time and temperature were studied. Results show that the aggregate contact with asphalt longer has higher apportion. Especially, the immersing time can affect the asphalt absorption dramatically. Temperature may also change the asphalt absorption, this can be attributed to the asphalt viscosity decrease at high temperature. Additionally, a model calculating the asphalt absorption over time was also proposed.

Second, the density gradient column method was applied to the loose-mix materials, investigating the absorption of warm mix asphalt. Also, the loose-mix asphalt binder was extracted and recovered to evaluate its chemical and physical properties, which were finally compared with asphalt absorption. A theoretical absorption model covering these properties was also discussed.

Introduction

Asphalt absorption is a dynamic process where contact time and temperature each play important roles. Thus, a study of the effect of contacting conditions on absorption is necessary. The density gradient column can be adopted as an efficient method for exploring absorption fundamentals, including the effects of time (both mixing and curing) and temperature. Following the steps that occur in the hot-mix (or warm-mix) coating and curing process, the density gradient column method requires aggregates to be immersed in asphalt for a specified period of time at a specified temperature and then cured in an oven at a different temperature for a much longer time period. In previous chapter, the mixing time and curing time of asphalt are standardized. However, the effects of the contacting time and temperature on the final asphalt absorption value are uncertain, calling for a systemic evaluation.

Meanwhile, asphalt absorption on clean aggregate using well-controlled laboratory conditions and the DGC method has been demonstrated in the previous chapter. Yet direct absorption measurements of mixtures are needed to provide a calibration of mixture processes to laboratory methods and to compare actual technologies (such as WMA), as implemented in the field, to conventional methods. The field and proprietary aspects of commercial processes provide their own challenges to duplicating field results in the laboratory and thus necessitate a valid measurement on the field mixtures.

Density gradient column, as a more precise way to study asphalt absorption, has the capacity to investigate the asphalt absorption in each single aggregate piece. Thus

promising convenient measurement on multiple conditions to study the potential factors controlling asphalt absorption. In this chapter, the density gradient was applied to study the asphalt absorption under various contacting condition and the absorption of loos mix materials. Besides, asphalt absorption models (both empirical and theoretical) addressing the contacting condition and materials properties were developed and discussed.

Objective

There were three primary objectives of this work:

- To study asphalt absorption under different preparation procedure, and develop a model to calculate the asphalt absorption over time.
- To directly measure the level of asphalt absorption achieved in loose mixes samples

Materials and methods

Materials

The materials for the time and temperature experiments were Jones Mill quartzite aggregate and Lion 64-22 asphalt binder. A single Lufkin district pavement site was used for the loose-mix study. The warm mix technologies placed in Lufkin sample were Sasobit, Evotherm DAT, Akzo Nobel Rediset, and Advera.

Characterization

Two analytical techniques were used to characterize the oxidation level of unaged and aged binders. Infrared spectroscopy was used to measure the carbonyl area as discussed in the literature review. A Carri-Med CSL 500 controlled-stress rheometer was used to measure both the low-shear-rate limiting viscosity and the DSR function.

The low-shear-rate limiting viscosity is obtained from a frequency sweep at 60 ℃ from 0.1 rad/s to 100 rad/s. The DSR function is measured at 44.7 ℃ and 10 rad/s then time-temperature shifted to 15 ℃, 0.005 rad/s [45].

Density gradient column for loose mix

Asphalt absorption addressing the contacting time and temperature variance are following the previous density gradient column procedure, while the absorption measurement of the loose mix are slightly revised:

To measure the absorption of loose-mix asphalt by DGC, a reverse process was applied. This process is the reverse of the method described in the previous chapter because the coated aggregate is measured first; then the aggregate is characterized after it is stripped of the binder. Specifically, the steps are:

- Measure the mass and density of the aggregate coated with asphalt.
- Extract and recover the aggregate with THF solvent.
- Measure the cleaned aggregate bulk density and apparent density using the wax coating and water-saturation methods described and applied in Chapters II.
- Adjust the binder density with any filler aggregate mixed with asphalt.

The reverse process necessarily started with measuring the density of the binder-coated aggregate followed by stripping the aggregate of coated and absorbed binder and then measuring the aggregate bulk and apparent densities. These aggregate densities, together with the recovered binder density, were used in the DGC method calculation. Measuring the binder density was complicated by the presence of fillers in the mix. A

calculation procedure based on measuring the recovered binder (but absent filler) density and mass and the recovered filler mass was used to estimate the binder/filler density that existed in the mixture.

Result and discussion

Asphalt absorption procedure in DGC method

As described in Chapter II, in the DGC experiment, asphalt was applied into the clean aggregate pieces through two steps. Figure 10 shows a schematic diagram of this two-step asphalt absorption procedure. First step was 143℃ mixing, when aggregate pieces were dropped into melted asphalt, immersed and stirred for certain period of time (15 s). In the second step, the aggregate pieces (after 15 s of immersed mixing, coated with asphalt) were taken out from the mixing beacon of melted asphalt and placed into a constant-temperature oven (143℃) to proceed a subsequent curing process (2 h). Contacting conditions such as time and temperature, were supposed to affect the final absorption value. Chapter II showed that DGC can provide precise result of asphalt absorption in porous aggregate, promising the opportunity to better understand the fundamental of this absorption process. Thus, a study regarding the effects of contacting conditions (i.e., time and temperature) on asphalt absorption are presented in the following sections.

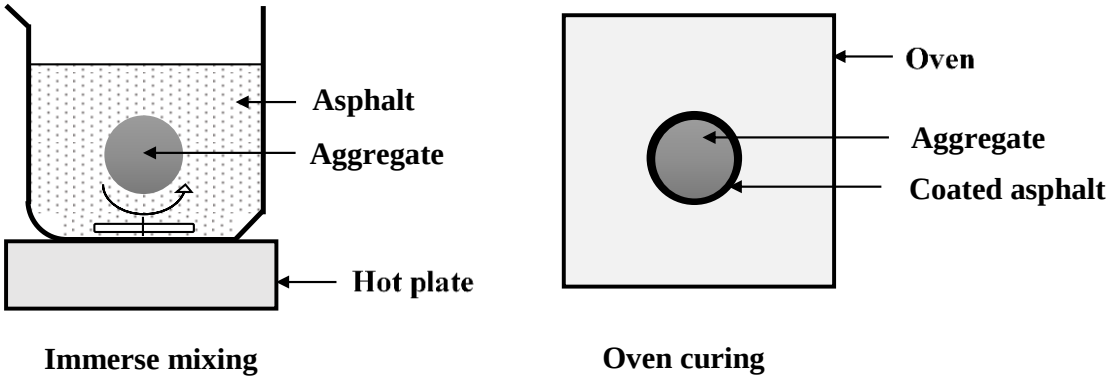

Figure 10. Schematic diagram of asphalt absorption procedure in DGC

Contacting time and asphalt absorption

The effect of mixing time on asphalt absorption was evaluated using multiple (from four to eight) pieces of one aggregate type (Jones Mill quartzite) and one asphalt binder (Lion PG 64-22). All aggregates were immersed in the well-stirred asphalt at 143℃, for five periods: 15 s, 1, 3, 5 and 10 minutes. After immersion, these aggregates were quenched in cold water (room temperature) for 1 min to stop the absorption process and measured immediately. Figure 11 and Figure 12 show the fraction of aggregate void occupied by asphalt during the trial time period. Clearly, aggregate has a high capacity to fill a large fraction of the aggregate void with asphalt, given a sufficient contact time while totally immersed in asphalt. After 10 min, the asphalt fills nearly 90 % of the available voids in the aggregate. On the other hand, after 15 s, the absorption is greatly less than it is after10 minute, and only a little over one-fourth of the 40 % value obtained during the baseline test of 15 s plus 2 h cure time. Evidently, there is significant absorption that occurs while the mixture is hot but after the coating process.

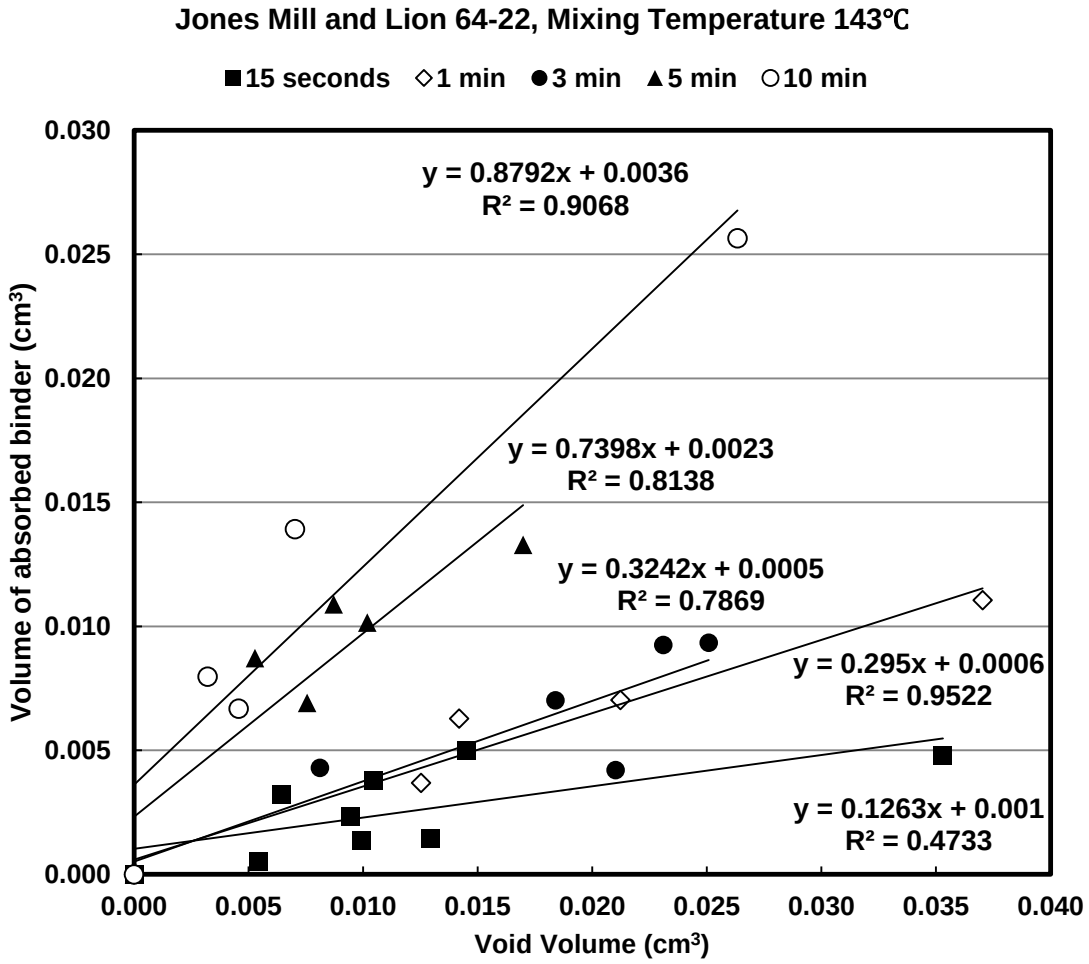

Figure 11. Linear correlations of void volume and absorbed asphalt volume at different mixing times.

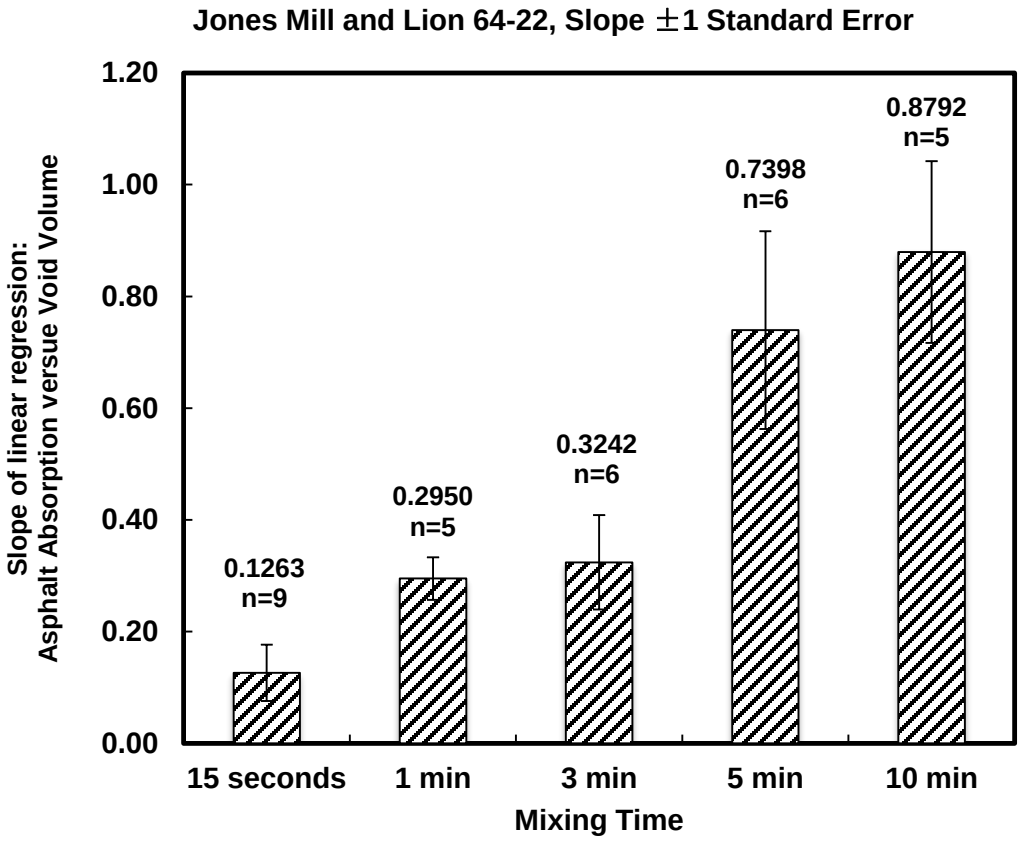

Figure 12. Statistical analysis of asphalt absorption and mixing time.

Also, a series of tests were conducted to evaluate the effect of curing time (after immersing the aggregate in hot asphalt) on asphalt absorption. All aggregates were pre-immersed under Lion 64-22 asphalts for 15 seconds at 143℃ and then further cured in a constant temperature oven at 121℃. The curing times are 0.5 and 2 hours (

Figure 13 and Figure 14). Additional data were obtained to fill in the time gaps and establish the progression of absorption over time (Figure 15). At these conditions, approximately 1 h is required to approach the baseline absorption level of 0.4 aggregate void fraction filled with asphalt. And, an extended curing time experiment up to 5 h

show that the asphalt absorption value stay around 0.4, after the initial increase of absorption level. This result suggested that for 15 seconds mixing, asphalt absorption under the curing condition may reach a "saturation" status after 1 h and under this status, around 40 % of the void volume in aggregates is occupied by asphalt binder.

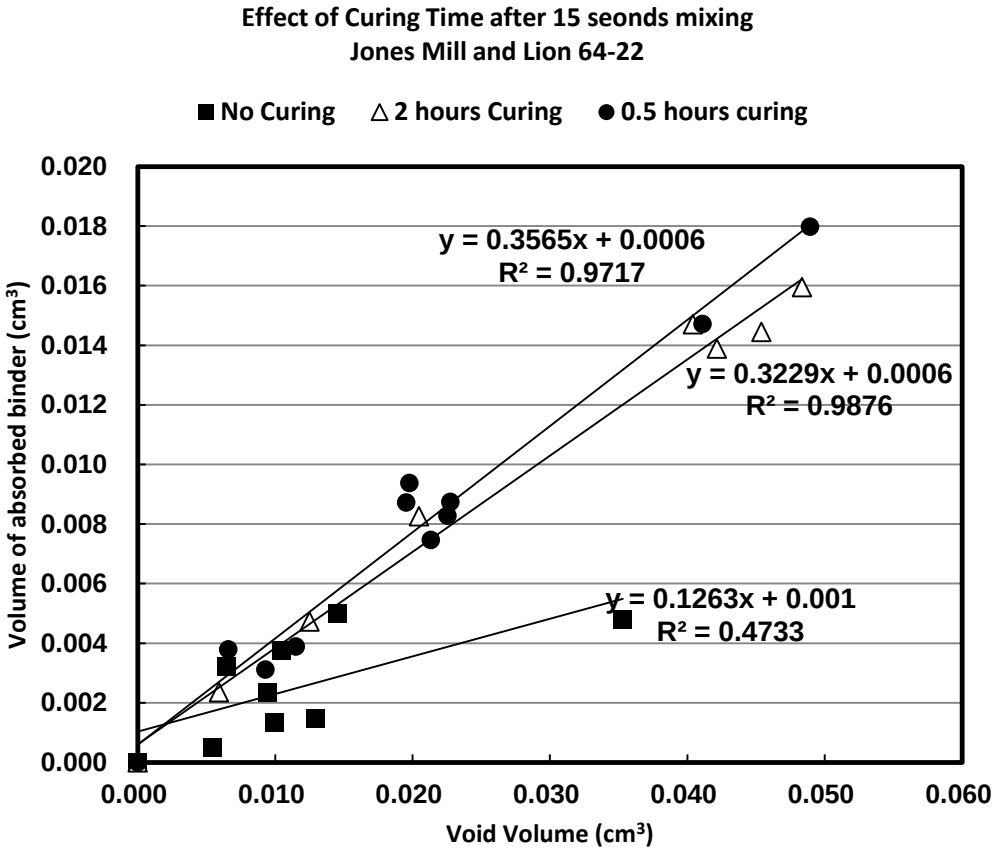

Figure 13. Linear correlations of absorbed asphalt and volume of air voids on different curing time at 121℃.

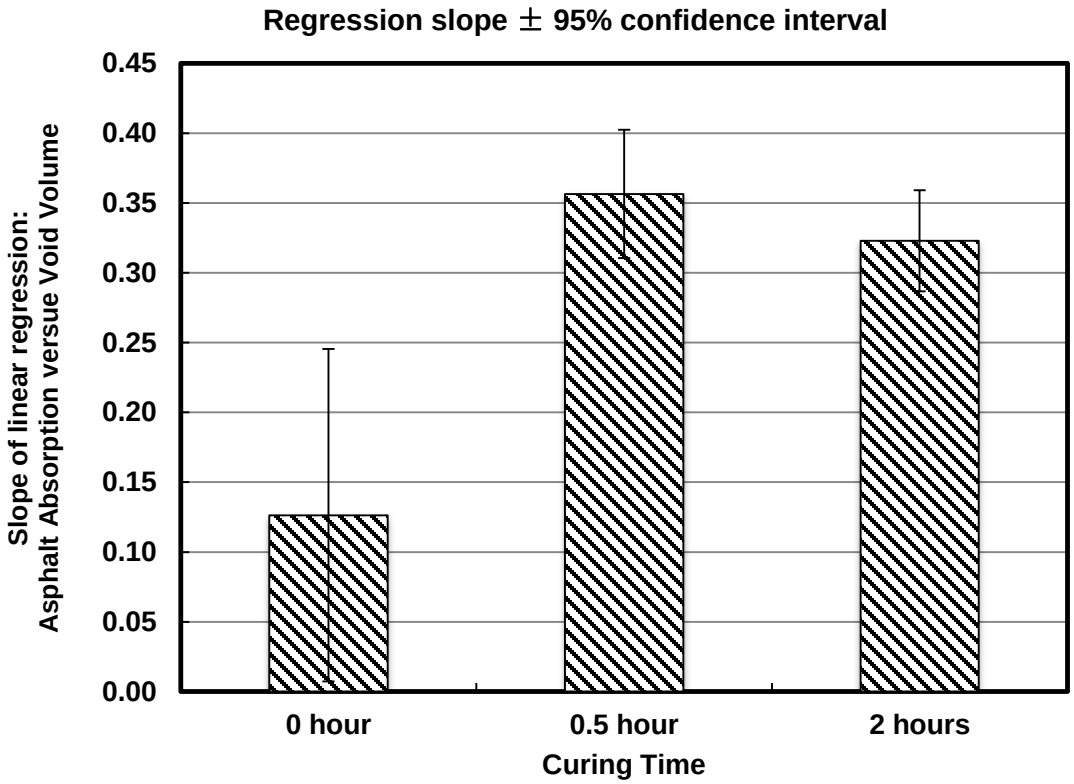

Figure 14. Statistical analysis of the volume fraction of air voids occupied by asphalt.

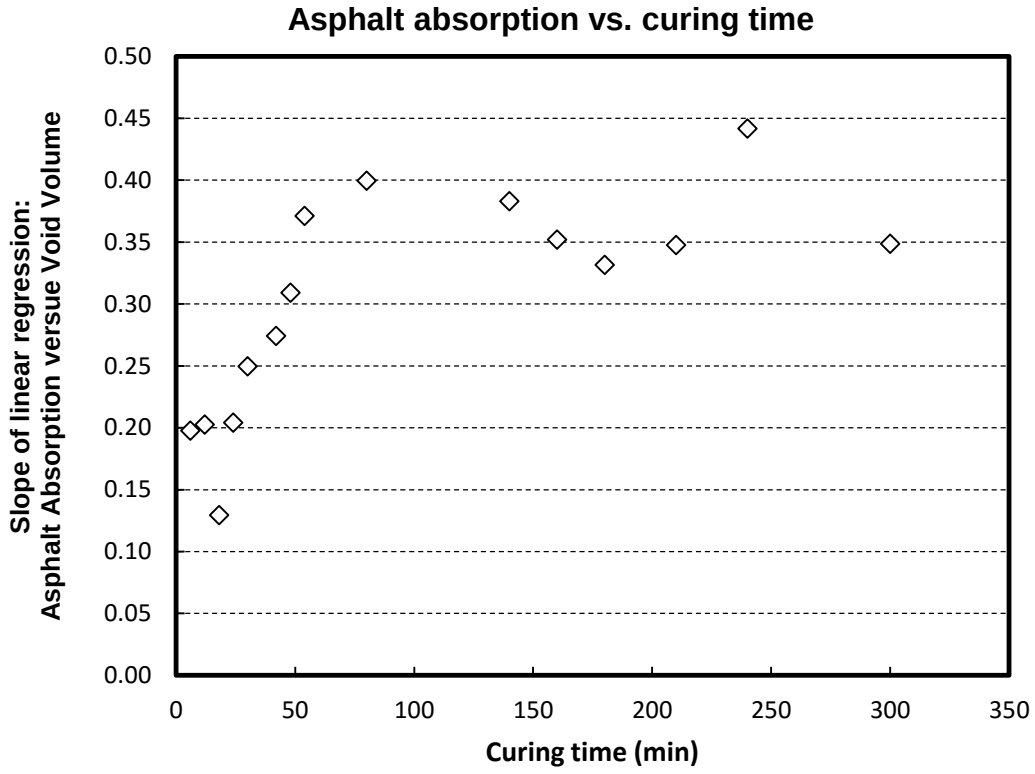

Figure 15. Curing time and asphalt binder absorption (curing at 121 ℃, after 15 seconds mixing).

Comparing with the mixing time result, it is clear the asphalt absorption under curing condition happens much slower. This difference in absorption rate is reasonable: First, when mixing, the aggregate are completely immersed into melted asphalt while well stirred. This immersion increase the contact of asphalt and aggregate; as well as providing a higher pressure at the asphalt/aggregate boundary. Additionally, it can be expected that the higher temperature (143 ℃) at mixing also contributed to more absorption. Interestingly, the immersed mixing absorption does not show a clear upper limit of absorption level like the curing time results. From Figure 11 and Figure 12, it

can be expected that the asphalt may eventually occupy all the void volume, if the time is long enough (10 min immersion mixing already lead to above 80%). This result suggests that the asphalt absorption might have undergone different mechanisms, from immersed mixing contact to non-immerse curing contact. During and after pavement construction, the "curing type" absorption might be the real case, considering the relatedly low binder content (around 5 % by weight, which is insufficient to immerse the aggregates) in pavement mixture.

Temperature and asphalt absorption

Beside contact time, another factor may affect asphalt absorption would be the contact temperature. To evaluate this temperature effect, asphalt absorption under different contacting temperatures (on a range of 40℃, covering the hot mix and warm mix preparation temperatures) were measured by density gradient column. Like previous DGC experiments, the contacting time here were fixed to be 15 s mixing and 2 h curing. Table 6 shows the effect of temperature on asphalt absorption. Results suggest that high temperature leads to more asphalt absorption, the reason could be a lower viscosity at high temperature. Warm mix asphalt technology required a lower temperature during the pavement mixture preparation, which might reduce asphalt absorption. However, the additives of the warm mix might also alter other properties of asphalt (surface energy, viscosity, etc.), so merely temperature results were not sufficient to make a conclusion of warm mix asphalt absorption. It is also notable that the effect of temperature on asphalt absorption is not very significant, comparing to the effect of time. One possible reason is the temperature range covered in this DGC experiments (40℃) is not large enough to

show impact as strong as contacting time. It is very challenging to further expand this temperature range, because it difficult to melt the asphalt at lower temperature.

Table 6. Effect of mixing and curing temperature on asphalt absorption.

Contact Temperature		**Asphalt Absorption**
Mixing (℃), 15 s	Curing (℃), 2 h	$V_{abs\text{-}b}/ V_{void}$
163	141	0.3260
143	121	0.3126
123	101	0.2602

Loose mix asphalt absorption

Additionally, the density gradient column method was applied to measure the asphalt absorption in Lufkin loose-mix samples. As previous experiments, this loose-mix sample study was done on a piece-by-piece basis. During the absorption experiment, other relevant aggregate properties, such as bulk density, apparent density and void volume were also measured. Table 7 shows data from DGC method for the Lufkin loose-mix samples.

Table 7. Lufkin loose mix asphalt absorption

Asphalt Type	Mass of Aggregate	Bulk Density (g/cm^3)	Apparent Density (g/cm^3)	Void Volume (cm^3)	Void Fraction	Volume of absorbed binder (cm^3)
Control	1.2920	2.561	2.891	0.057	0.1140	0.027
Control	1.2176	2.593	2.835	0.040	0.0851	0.018
Control	0.8616	2.593	2.802	0.025	0.0746	0.009
Control	1.0465	2.594	2.876	0.040	0.0980	0.015
Control	0.3154	2.484	3.066	0.024	0.1900	0.009
Sasobit	0.2472	2.529	3.036	0.016	0.1670	0.010
Sasobit	0.6119	2.567	2.942	0.030	0.1277	0.013
Sasobit	0.2745	2.586	2.912	0.012	0.1119	0.004
Sasobit	1.0202	2.503	3.057	0.074	0.1814	0.029
Sasobit	0.4809	2.489	2.973	0.031	0.1629	0.013
Sasobit	0.2839	2.548	2.828	0.011	0.0990	0.006
Sasobit	0.4049	2.476	3.073	0.032	0.1943	0.014
Sasobit	1.0239	2.506	2.980	0.065	0.1592	0.028
Sasobit	0.6589	2.573	2.916	0.030	0.1176	0.014
Sasobit	0.6560	2.507	3.034	0.045	0.1736	0.018
Evotherm	0.3720	2.493	3.098	0.029	0.1953	0.010
Evotherm	0.5176	2.478	3.055	0.039	0.1889	0.013
Evotherm	0.6507	2.326	3.321	0.084	0.2996	0.028
Evotherm	0.5346	2.417	2.963	0.041	0.1843	0.011
Evotherm	0.1741	2.501	3.017	0.012	0.1711	0.005
Evotherm	0.5748	2.534	2.981	0.034	0.1501	0.012
Advera	0.4775	2.469	2.765	0.021	0.1070	0.007
Advera	0.8093	2.557	2.900	0.037	0.1183	0.009
Advera	0.3627	2.513	2.972	0.022	0.1546	0.006
Advera	0.6297	2.581	2.885	0.026	0.1054	0.007
Advera	0.5647	2.499	2.932	0.033	0.1474	0.007
Advera	1.1301	2.525	2.972	0.067	0.1506	0.018
Advera	0.4978	2.522	3.038	0.034	0.1700	0.010
Advera	0.6371	2.595	2.814	0.019	0.0777	0.002
Rediset	0.4464	2.630	2.805	0.011	0.0623	0.003
Rediset	0.9930	2.528	2.865	0.046	0.1176	0.016
Rediset	0.3152	2.574	2.814	0.010	0.0855	0.003
Rediset	0.6356	2.557	2.821	0.023	0.0936	0.009
Rediset	0.2835	2.641	2.778	0.005	0.0493	0.002
Rediset	0.2728	2.582	2.785	0.008	0.0729	0.002
Rediset	0.3003	2.488	2.882	0.016	0.1367	0.005
Rediset	0.5293	2.550	2.934	0.027	0.1310	0.009
Rediset	0.5085	2.625	2.795	0.012	0.0607	0.003
Rediset	0.6220	2.531	3.010	0.039	0.1592	0.010

DGC measurements indicate that the volume of asphalt absorption correlates well with the void volume, for all types of loose mix samples (both hot mix asphalt and warm mix asphalt). However, the slope of this correlation for the different mixtures varies, suggesting that warm mix asphalt has different asphalt absorption level. Figure 16 and Figure 17 show these results.

The dominant feature of these absorption measurements is that in each case, the WMA loose mixtures exhibited less absorption than the HMA control. The difference between the control and Sasobit mixtures could be considered not significant ($p = 0.09$) but the differences from the control mix are much better defined for the other WMA processes (Evotherm: $p = 0.008$, Advera: $p = 0.002$, Rediset: $p = 0.01$).

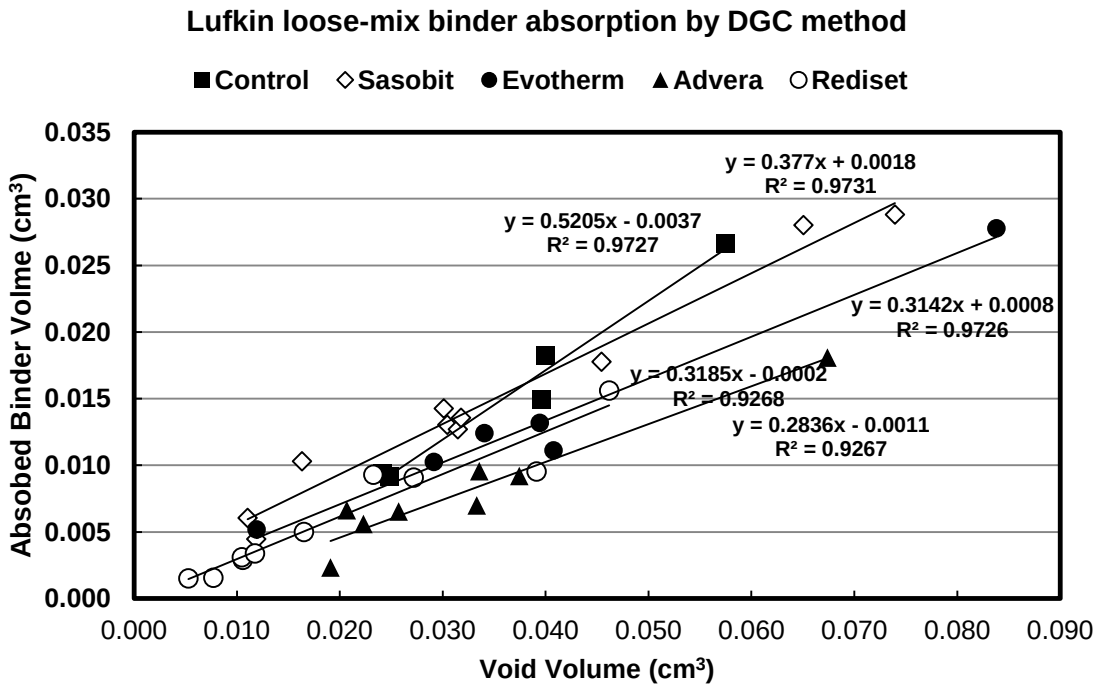

Figure 16. Linear correlations of asphalt absorption and air void, volumetric view.

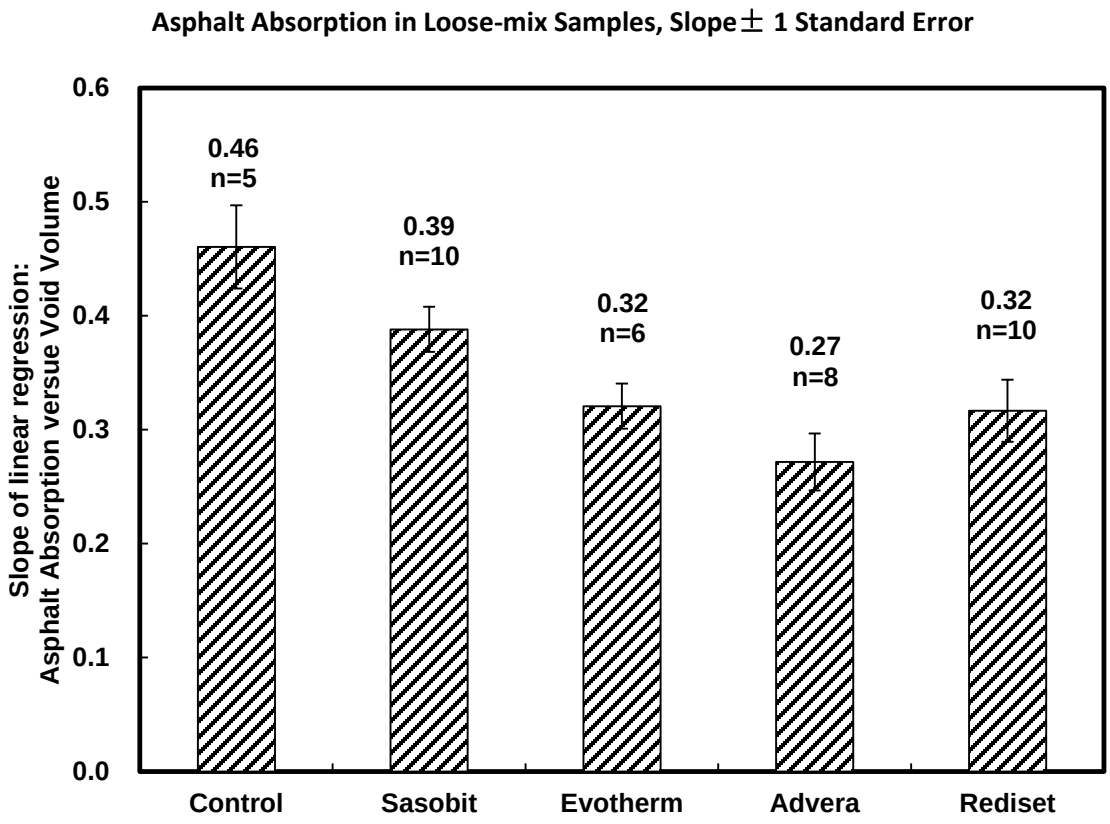

Figure 17. Summary of loose mix asphalt absorption.

Recovered loose mix asphalt properties

After extraction and recovery by THF/toluene solvent, asphalt binders are successfully recovered from Lufkin loose mix. Subsequently, mechanical and chemical properties (the DSR function, the 60℃ low-shear-rate limiting viscosity, and the FTIR carbonyl area) of these recovered asphalt binders were measured (Table 8).

Table 8. Characteristics of Recovered Lufkin Binder.

Asphalt Type	60 ℃ Limiting Viscosity	DSR Function	Carbonyl Area
HMA Control	13770.04	0.000070	0.877
Sasobit	18328.64	0.000096	0.888
Evotherm	21935.24	0.000133	0.924
Advera	20761.36	0.000130	0.945
Rediset	15999.90	0.000071	1.009

As an exploration to the factors affecting asphalt absorption, these binder properties were compared with the asphalt absorption data. Interestingly, linear correlations of the various recovered binder properties (log low-shear rate viscosity, log DSR function, and CA) with binder absorption (expressed as volume of binder absorbed per aggregate void volume) were found for the HMA control, Sasobit, Evotherm and Advera asphalts (Figure 18, Figure 19 and Figure 20).

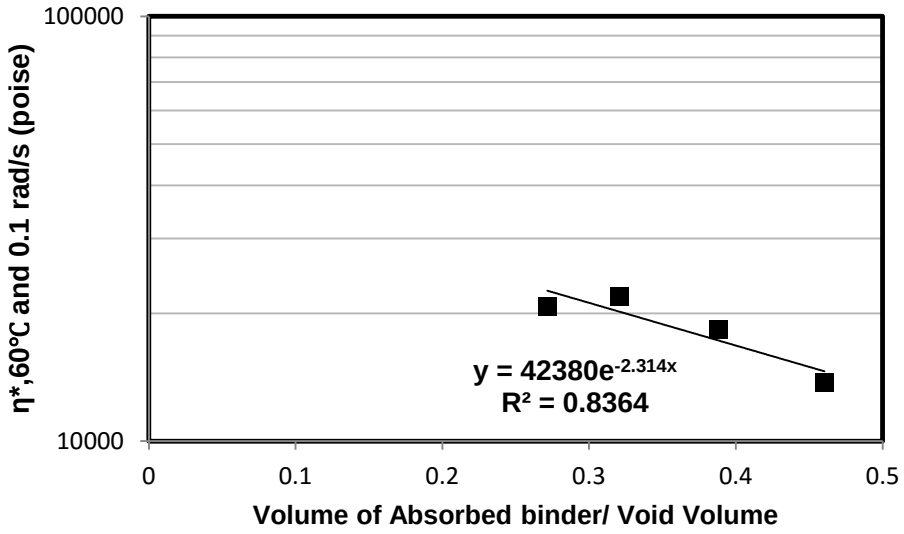

Figure 18. Exponential correlation of absorption fraction and 60℃ limiting viscosity.

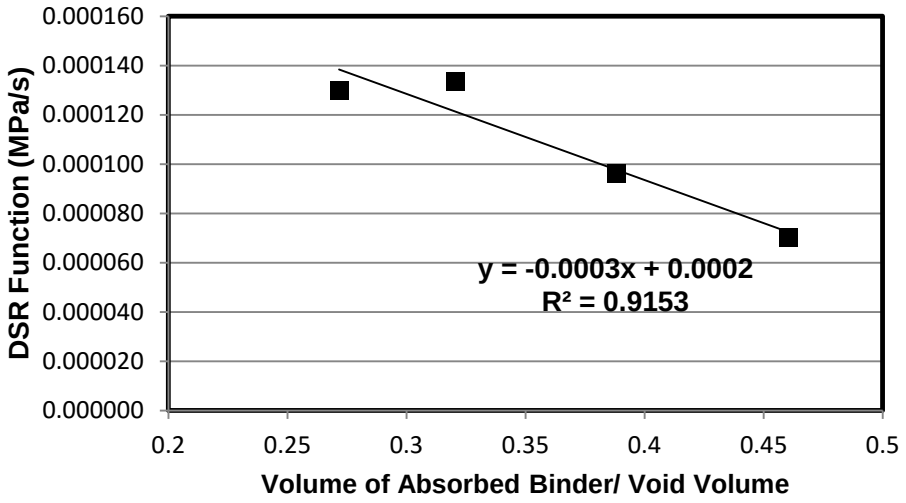

Figure 19. Linear correlation of absorption fraction and DSR function.

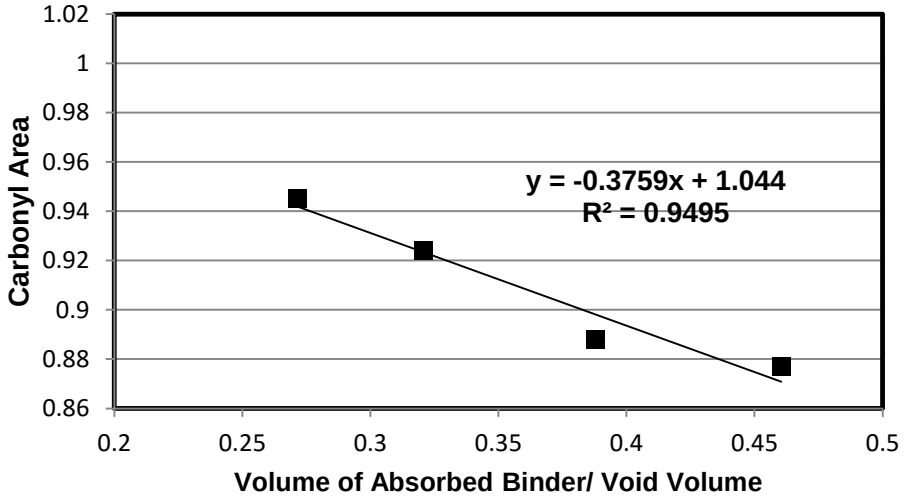

Figure 20. Linear correlation of absorption fraction and carbonyl area value.

These correlations suggested that more aged binder appears to show lower absorption. It would make sense that the less "stiff" the binder rheology (expressed either as the 60℃ low-shear-rate limiting viscosity or as the DSR function), the higher the absorption, and indeed, this is the case. Plus the fact that CA also shows a correlation is simply a reflection of the HS relation between the binder rheology and oxidation level. However, what does not seem to fit is the fact that the HMA binder is the binder that is less "stiff" and less oxidized, rather than the WMA binders. Furthermore, we would expect that the lower WMA processing temperatures (compared to the HMA process) would result in reduced asphalt absorption for the WMA process. And, it may well be true that without the reduced temperature, the binder absorption differences in the loose mix samples would have been even more accentuated than the data show. Rediset binder does not fit these correlations as the other binders, as the Rediset binder appears to have a lower absorption. This might be attributed to the special chemical composition of Rediset technology. This extraordinary data point also suggested that the relation found here may not be generalized to all warm mix asphalt binders yet.

Empirical asphalt absorption model

A quantitative model used to estimate the asphalt absorption over time has been reported in literature [13], and the governing equation is:

$$A = A_0 + \frac{t}{a + bt} \tag{11}$$

where A is the asphalt absorption (by weight percent of aggregate) at time t, A_0 is the asphalt absorption at time zero, a and b are two constants calculated based on the absorption measurement at two more aging times.

A revised model based on Equation (11) was developed to fit the DGC asphalt absorption data under different curing times, where the indicator of asphalt absorption level was replaced from mass base (weight percent of aggregate) to fundamentally more reasonable volumetric base (fraction of air void occupied by asphalt). As an example, least square fit of this absorption model based on the absorption data shown in Figure 15 provides the following equation with optimized regression parameters:

$$A = 0.1038 + \frac{t}{99.55 + 3.147t} \tag{12}$$

where A is the asphalt absorption (volume fraction of air void occupied by asphalt), t is the curing time (min). R^2 of this fit is 0.7355.

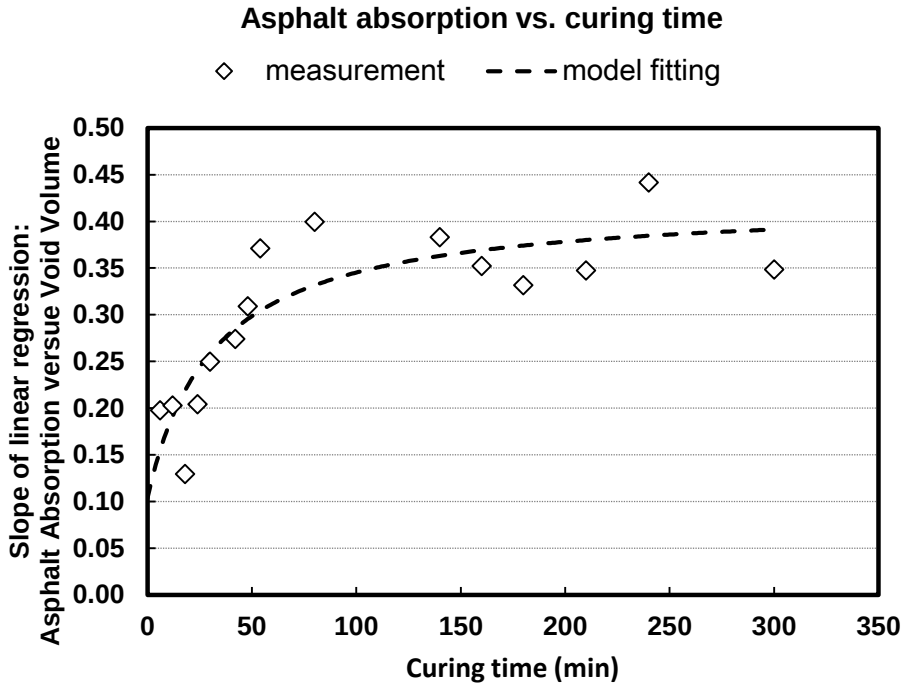

Figure 21. Model fitting: curing time and asphalt absorption.

Figure 21 shows the model fitting results and the experimental data. This fitting result is very interesting. When curing time equals to zero, the asphalt absorption is 0.1038, very close the number given by previous mixing time experiment (where 15 s mixing without curing provides 0.1263); on the other hand, if the curing time is long enough (where *t* approaches infinite), the final absorption value could be 0.4215. This result suggests that by fixing the mixing time to 15 seconds, the saturation asphalt absorption level of 121℃ curing would be around 0.4, which is coherence with the previous chapter where the asphalt absorption of all six types of aggregates finally reach a level around 0.4.

Figure 12 shows a similar optimization was done based on the mixing time data. As the DGC experiment started with clean aggregates, the initial absorption level in mixing time experiment was zero, which means A_0 equals zero in the mixing time model. Based on this concept, the following equation was generated:

$$A = \frac{t}{4.16 + 0.7093t} \tag{13}$$

where A is the asphalt absorption (fraction of air void occupied by asphalt), t is the mixing time (min). R^2 of this fitting is 0.8915.

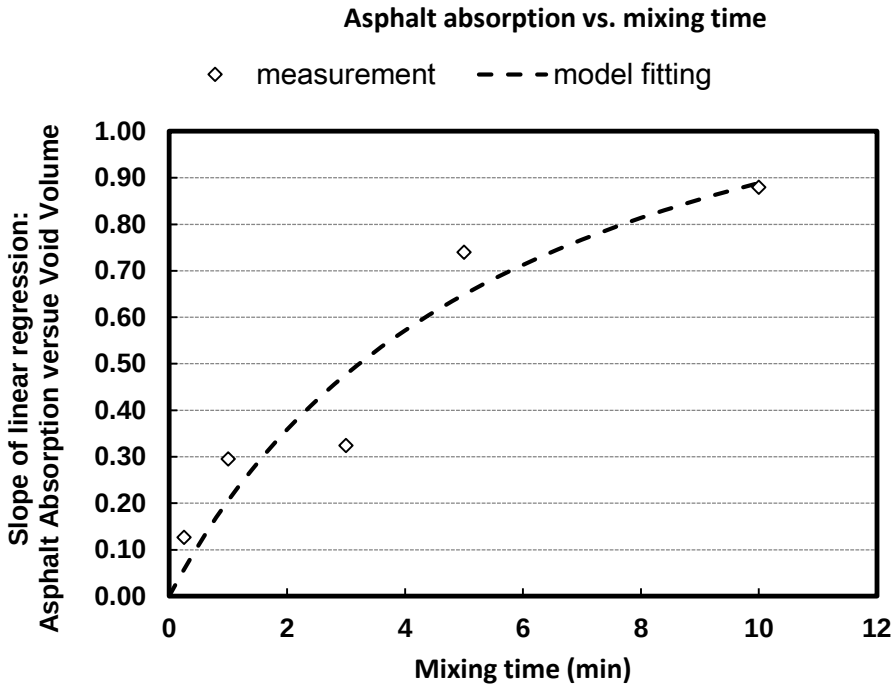

Figure 22. Model fitting: mixing time and asphalt absorption.

Model fitting on mixing time shows that its effect on asphalt absorption is much more significant than curing time. Possible reasons include: (1) mixing procedure has a higher temperature; (2) when the asphalt was immersed into stirring melted asphalt, there were better contact, lower viscosity and more pressured asphalt/aggregate interface. It is also notable that after 10 min of immersed mixing, the asphalt absorption are above 0.8, which means more than 80% the air voids volume are occupied by asphalt (i.e., water absorption volume). It is expected that if the immersed contact time is long enough, the asphalt could fill all aggregate pores, just like water did. This phenomena is different from the curing model, where the limitation is around 45 % of the air voids, suggesting that the mechanism of immersion absorption maybe different from the curing absorption, thus, to describe the asphalt absorption under different contacting time in the DGC experiments, a model incorporating these two steps separately could help.

A two-step model addressing these two different contacting conditions respectively was developed. The governing equation of this two-step absorption was:

$$A = \frac{t_m}{a_m + b_m t_m} + \frac{t_c}{a_c + b_c t_c} \tag{14}$$

where A is the asphalt absorption (fraction of air void occupied by asphalt), t_m is the mixing time (min), while t_c is the curing time (min). a_m, b_m, a_c and b_c are four constants could be optimized based on the absorption data.

Theoretical absorption mechanism

The fundamental of asphalt absorption process are viscosity liquid flowing into porous material. This process could be simplified as Figure 23, showing the pore radius, pore depth and the contact angle of asphalt aggregate interface. It is notable that depending on the wetting angle and pressure gradient, the asphalt/air interface curves could show different shapes. Figure 23 showed the three possible cases, while the following calculation were based on one possible case, in which there was a "C" shape asphalt/void interface.

A theoretical model was developed to describe the asphalt absorption process regarding Figure 23. The pores in aggregates are assumed to be cylindrical tubes. Additionally, the effects of aggregate pore size, asphalt viscosity and capillary force were incorporated into this absorption model. The governing equation of this absorption model is:

$$\frac{V_{abs-b}}{V_{void}} = \sqrt{\frac{2r(\Delta G)(\cos\theta)}{3L^2(\mu)}(t)} \tag{15}$$

where r is the diameter of air void, L is the air void depth, ΔG represent the surface energy tension among asphalt and aggregate, θ is the contact angle, μ is the viscosity of asphalt, t is time of absorption, $V_{abs\text{-}b}$ is the volume of absorbed asphalt, and V_{void} is the air void volume.

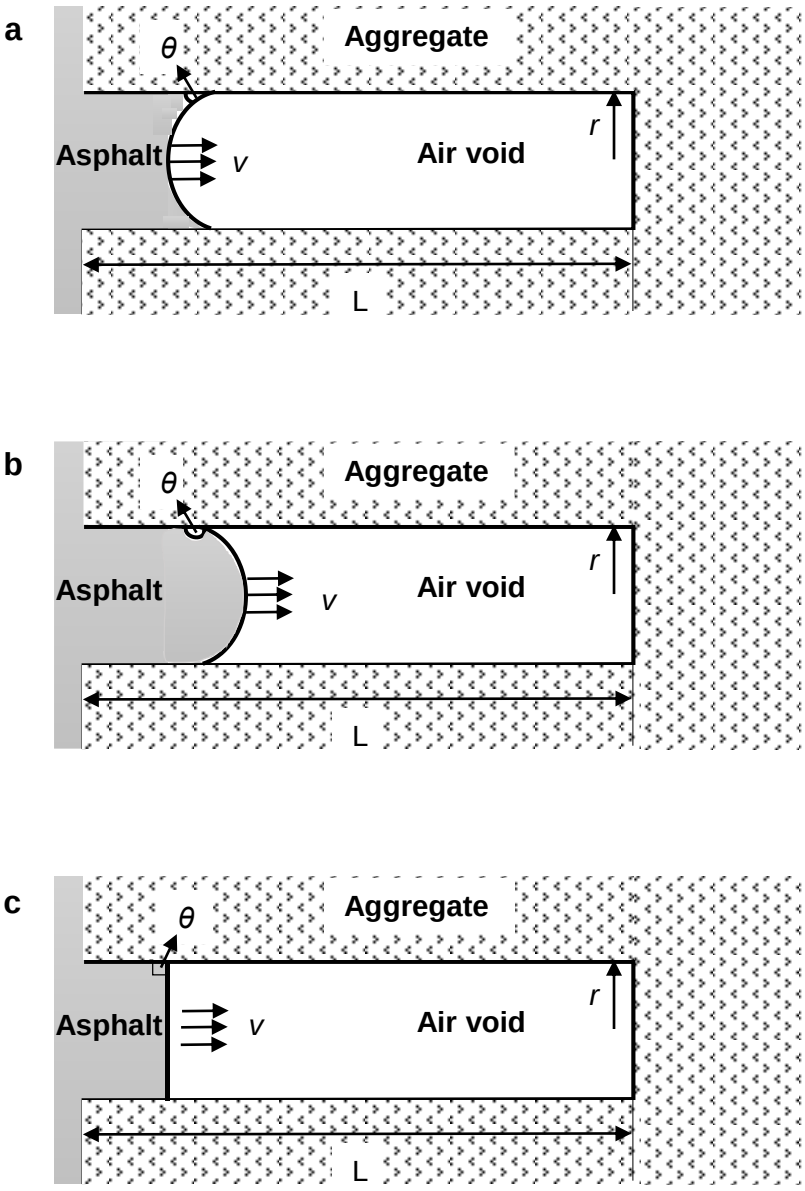

Figure 23. Schematic diagram of asphalt flowing into aggregate pores.
(*r:* pore diameter, *L:* pore depth, θ: contact angle, *v*: velocity of asphalt)

This model proposed that the absorption is related to air void, time, pore size, surface energy and viscosity. Refer to asphalt absorption results from Chapter II, volumetric based asphalt absorptions ($V_{abs\text{-}b}/V_{void}$) of six different aggregates types (supposed to possess different pore sizes and surface properties) were very closed to a universal 40 %. This result suggested air void volume as a dominating factor, comparing to other aggregate properties. Contacting time results also indicated that after 15 seconds of immersed mixing and 2 hours oven curing, the aggregate pores were "saturated". It is possible that factors like aggregate viscosity and surface energy mainly affected the initial absorption speed, but their effects on the long term absorption (when the air voids in aggregate were "saturated") were less significant.

Conclusion

This fraction of the aggregate void volume occupied by absorbed asphalt has been established as a fundamental factor to understanding the effects of time and temperature on absorption. It's not surprising that as the contact time increases, asphalt absorption increases, and vice versa. When an aggregate is immersed into asphalt for more than 5 minutes, more than 70 % of the air voids were filled with asphalt. Curing aggregate with asphalt at 121℃ can also increase the asphalt absorption, but at a much slower rate than that at higher temperatures. Temperature experiments evaluated absorption at three different temperatures over a 40℃ range. Basically, higher temperatures will cause more absorption, most certainly because of the reduced asphalt viscosity at higher temperatures. Based on these results, less absorption might be

expected in WMA because of the lower temperatures, with the caveat that WMA additives may well alter the absorption trends.

By reversing the process of density gradient column, asphalt absorption in loose mixes was measured. This test covered several warm mix asphalt binder and their base binder control. As with the previous asphalt absorption results, loose mixture measurements also found that binder absorption depends linearly on aggregate void volume. This result supports the conclusion that void volume is a fundamental factor in establishing asphalt absorption. Interestingly, consistent with the temperature experiment, the WMA loose mixes exhibited less absorption than the HMA control, as WMA has a lower contacting temperature. As an exploration, various recovered binder properties (log low-shear rate viscosity, log DSR function, and CA) were determined and compared with the asphalt absorption (expressed as volume of binder absorbed per aggregate void volume). The data suggested that the binder stiffness maybe related to the asphalt absorption, for certain types of asphalt binders.

Asphalt absorption model is also discussed in this chapter. First, based on literature report, an empirical model describing the asphalt absorption over time was developed and discussed. This model fit the asphalt absorption results under different contacting time very well. Also, it is highly possible that the asphalt absorption follows two different mechanisms, for immerse mixing and oven curing. Second, a theoretical model addressing the aggregate and asphalt properties was proposed. A discussion of this model based experimental results suggested that air void and time may be the dominating factor in asphalt absorption process.

CHAPTER IV

A STUDY ON THE OXIDATION KINETICS OF WARM MIX ASPHALT*

Warm mix asphalt (WMA) is increasingly used in pavements to reduce energy consumption and emissions, and to extend workability times. Literature reports on warm mix asphalt have addressed its usage, but its oxidation kinetics and possible effects on pavement durability are unknown. In this work, several popular types of WMAs were used in multi-temperature experiments to estimate oxidation kinetics parameters of an Arrhenius reaction model. Additionally, an example pavement aging simulation explored the potential effects of differences in activation energy on pavement aging.

Constant-rate activation energies show statistically insignificant differences between the base binder and its WMAs; additionally, for each WMA material all four kinetics parameters follow the same correlations previously established for 15 non-WMA binders. These results suggest no adverse effect of WMA additives on asphalt oxidation, compared to the base binder. An example pavement binder oxidation simulation specific to Lubbock, Texas indicates that first, between a base binder and its corresponding WMAs, differences in pavement oxidation over 10 years of pavement service would be minimal and second, oxidative hardening may (or may not) slow the overall reaction rate as diffusion resistance increases, depending on the balance between diffusion and reaction rates.

*This chapter is reprinted with permission from "A study on the oxidation kinetics of warm mix asphalt" by Guanlan Liu, Charles J. Glover, 2015, *Chemical Engineering Journal*, Vol. 280, 115-120. Copyright 2015 by Elsevier.

Introduction

Warm mix asphalt (WMA) technologies, with significantly reduced mixing and compacting temperature, have been attracting increased attention in recent years. Deploying WMA technology in the asphalt industry promises economic benefits (reduced fuel consumption and extended paving season) plus technical convenience (enhanced compaction and increased haul distances). Popular warm mix additives include emulsion-based additives, chemical additives, and synthetic additives. Much effort has been made towards understanding the effects of WMA technology on pavement performance [2-6]. In particular, warm mix asphalt oxidative aging resulting in pavement fatigue failure, is now recognized as an important factor in pavement design [46-48]. It has been shown that some warm mix asphalt binders demonstrated changed rheological behavior after long-term aging [47-49]. The driving force of these rheological changes is the chemical reaction of asphalt and oxygen, i.e., asphalt oxidative aging. Thus, quantitatively understanding oxidative aging and consequent hardening, is key to predicting changes in rheological behavior. However, previous studies of warm mix asphalt focused on mechanical properties for limited aging states (e.g., one short-term aging state and one long-term aging state) with no work on WMA oxidation kinetics [50-54].

A fundamental understanding of oxidation kinetics is important because of the significant role that oxidation plays in causing changes to asphalt physical and chemical properties, changes that lead to irreversible binder embrittlement and reduced pavement life [1]. On the other hand, understanding oxidation chemistry and kinetics is

complicated by the fact that the asphalt oxidative aging procedure is complex because of the diversity of molecular types and the variation of oxidation rate affected by temperature, pressure, chemical composition (specific binder), and oxygen diffusivity [55-58]. Because of its importance to pavement durability and complexity, the goal of understanding asphalt oxidation fundamentals has attracted significant work from researchers over several decades when many studies have been conducted to explore, describe and predict asphalt physicochemical properties and chemical reaction mechanisms [21, 25, 59-62]. One significant discovery is that the carbonyl area (CA), measured in the infrared spectrum as the absorbance peak area above the 1820 cm^{-1} baseline and from 1820 to 1650 cm^{-1}, has been reported to relate linearly to the amount of oxygen reacted with asphalt [23]. Furthermore, for each asphalt material, there is a specific correlation between the carbonyl area growth and rheological hardening (measured by the low shear rate viscosity or by the DSR function defined by Ruan et al., 2003, recently redefined and termed the Glover-Rowe parameter [22, 45, 63]), which links asphalt oxidation kinetics to rheological hardening. Additionally, studies showed that asphalt oxidation could be represented by two parallel reaction processes at constant temperature: a nonlinear fast-rate reaction path and a linear constant-rate path [1, 23]. A theoretical model to describe both of these processes, and a method for estimating the kinetics parameters of the model has been reported [25]. The kinetics parameters can be used in a pavement oxidation model to predict asphalt aging in pavements over time and as a function of depth, for climates of choice [64]. However, previous kinetics research

has focused only on hot mix asphalt materials with no reports on the oxidation kinetics of WMA materials.

Objective

The principle objective of this work was to study the oxidation kinetics of warm mix asphalt materials by aging a PG 70-22 base binder with and without warm mix additives and to assess the potential impact of differences on pavement oxidation using a pavement oxidation model. Changes in *CA* under multiple time/temperature combinations provided kinetics parameters to be used in a pavement oxidation kinetics model.

Materials and methods

Materials

An unaged polymer modified PG 70-22 binder was blended with three typical WMA additives (emulsion, chemical and synthetic zeolite). The supplier of these WMA additives are Evotherm, Rediset, and Advera. For binder preparation, the base binder was pre-heated in a 140℃ oven for 30 min and distributed into 1-L cylindrical metal containers. During the heating process, nitrogen was purged in to the oven to prevent binder oxidation. WMA additives were then blended for 5 min at recommended concentrations, as shown in Table 9. The same base binder was also included in all the following experiments as a control.

Table 9. Asphalt sample preparation.

Asphalt	WMA Additives	WMA Additive Concentration (weight percent of asphalt)	CA_{tank}
PG 70-22	N/A*	N/A*	0.559
PG 70-22	Emulsion	0.50 %	0.583
PG 70-22	Zeolite	0.25 %	0.552
PG 70-22	Chemical	0.25 %	0.541

*Note: * Base binder control without warm mix additives*

CA_{tank} values, representing initial aging states, are summarized in Table 9. The values of CA_{tank} ranged from 0.541 arbitrary units (a.u.) to 0.598 a.u., a much tighter range than has been previously reported for different base binders (and not unexpected considering that all materials in this study used the same base binder) [25].

Aging procedure

Asphalt oxidation was conducted in pressure oxygen vessels (POV) designed for more precise temperature control than conventional ovens. Asphalt binders were poured into 4 cm × 7 cm aluminum trays so that the mass of the binders on each tray was 2.4 ± 0.05 gram. The average thickness of the binder was close to 0.8 mm. It has been shown that this thickness adequately reduces oxygen diffusion resistance for kinetics measurements at constant temperature. Samples were kept on racks in four different POVs with 1 atm air, each at at a different temperature (333 to 371 K) for up to 90 days. Each POV was immersed in a continuously stirred triethlene glycol (TEG)/water constant-temperature bath, at 333, 346, 359 or 371 K, with temperature fluctuations of ± 0.6 K. Moreover, fresh preheated air was purged into the vessel to maintain the oxygen concentration of fresh air. As the binders in the POVs aged at different rates

corresponding to their temperatures, samples were collected for testing according to the schedule in Table 10.

Table 10. Sampling timeline for asphalt at different aging temperatures.

Aging Temperature (K)	Aging Time (days)
333	2, 5, 10, 20, 35, 55, 90*
346	1, 3, 5, 8, 15, 30, 50
359	1, 2, 4, 6, 10, 20, 30
371	1, 2, 4, 6, 10, 20

*Note: * 90 day test only performed on base binder and one warm mix asphalt binder*

Characterization

A Thermo Scientific Nicolet 6700 Fourier-Transform Infrared (FTIR) spectrometer with an attenuated total reflectance (ATR) zinc selenide prism was used to measure carbonyl (C=O) area. In this procedure, the asphalt sample was softened by heating on a hot-plate and then applied to the prism. The CA (arbitrary units), defined as the peak area above the 1820 cm^{-1} baseline and from 1820 to 1650 cm^{-1}, has been used as a direct indicator of asphalt oxidation that relates directly to changes in binder rheology [61, 65, 66].

Results and discussion

Carbonyl area and asphalt oxidation

CA values, were measured for asphalt samples aged to different times at different temperatures. Figure 24 shows the CA growth over time of the base binder and WMA binders. The CA growth for 15 asphalt binders at constant temperature has been

characterized as a non-linear fast-rate reaction in parallel with a linear constant rate reaction. CA growth of a PG 70-22 binder selected for this study, either with or without warm mix additives, was consistent with this fast-rate, constant-rate model. These CA values, together with the aging time and temperature, provided the necessary data for estimating the kinetics parameters for this kinetics model, described below.

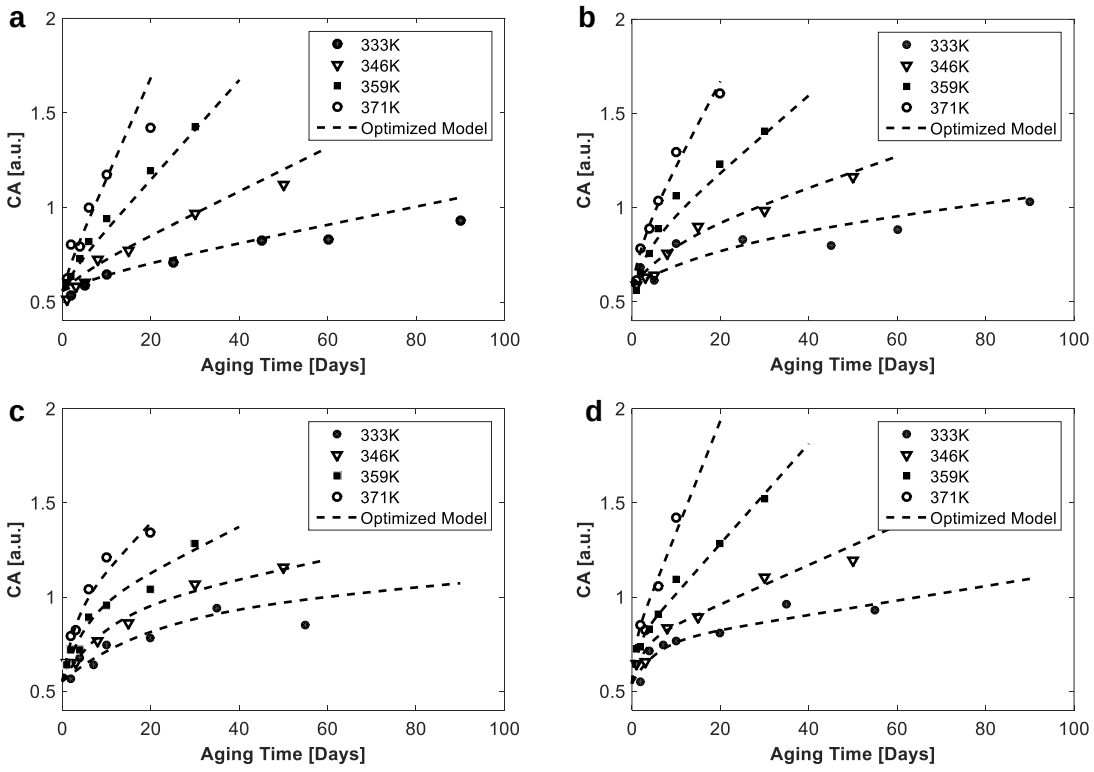

Figure 24. CA growth of asphalt binders at four temperatures in 1 atm air pressure (data: symbols; model calculation: dash lines): (a) base binder; (b) emulsion WMA binder; (c) zeolite WMA binder; (d) chemical WMA binder.

Kinetics model optimization

According to the fast-rate, constant-rate oxidation kinetics model [25], asphalt oxidation, represented by carbonyl area (*CA*) growth, can be described by the following equations reflecting the combined fast-rate, constant-rate parallel reaction processes:

$$CA = CA_{tank} + M\left(1 - e^{-k_f t}\right) + k_c t \tag{16}$$

$$k_f = A_f e^{-\frac{E_{af}}{RT}} \tag{17}$$

$$k_c = A_c e^{-\frac{E_{ac}}{RT}} \tag{18}$$

where CA is the carbonyl area of asphalt sample, CA_{tank} is the carbonyl area of unaged asphalt, $M=CA_0-CA_{tank}$ (CA_0 is the zero-time intercept of the constant rate reaction), k_f is the fast-rate reaction constant, k_c is the constant-rate reaction constant, A_f and A_c are pre-exponential factors for k_c and k_f, E_{af} and E_{ac} are the apparent activation energies for k_c and k_f, and R is the idea gas constant (8.314 J/(mol K)).

To evaluate possible effects of WMA additives on the reaction kinetics parameters, a mathematical optimization, using the reaction model described previously, was performed on the base and WMA additive treated binders. There are six parameters (CA_{tank}, M, A_f, A_c, E_{af}, E_{ac}) in this kinetics model, where CA_{tank} is measured directly for the unaged materials. The other five parameters are optimized using the reaction data [21]. In this research, the optimization was performed using multiple non-linear regression in Matlab®, where time and temperature are considered as two independent variables and *CA* is considered as the dependent variable. The dash lines in Figure 24 show the optimized model calculations for the base binder and for each WMA modified

binder, assuming a constant oxygen partial pressure of 0.2 atm and no diffusion resistance.

Parameter estimation summary and statistical analysis

Table 11 shows the optimized model parameter estimates for the base binder and WMA binders. Additionally, it has been reported that some WMA binders show less rheological hardening after aging [7] than conventional binders. One possible reason could be that these WMA additives slow the oxidation rate, but it's also possible that the hardening susceptibility, which reflects the impact of oxidation (CA) on the rheological properties of asphalt, may be altered by WMA additives.

Table 11. Optimized kinetics parameters for base binder and WMA binders.

Asphalt Binder	**Optimized Regression Coefficients**				
	A_f *(1/day)*	E_{af} *(kJ/mol)*	A_c *(1/day)*	E_{ac} *(kJ/mol)*	*M (a.u.)*
Base	1.34×10^{7}	52.45	7.87×10^{7}	65.12	0.0622
Emulsion WMA	9.92×10^{6}	52.84	6.16×10^{8}	72.01	0.1926
Zeolite WMA	4.00×10^{6}	50.24	8.71×10^{7}	67.77	0.3412
Chemical WMA	2.10×10^{7}	51.28	1.54×10^{9}	73.97	0.2104

Note: Model coefficients were estimated by multiple non-linear regressions in MATLAB curve fitting tool.

To evaluate the precision of the combined kinetics data and optimization procedure, statistical analysis was done on the parameters; the results are shown in Table 12. For the four data sets, SSE values ranged from 0.06 to 0.11, R^2 and RMSE values were above 0.92, and below 0.07 respectively. In addition, 95 percent confidence interval values for the constant rate activation energies (E_{ac}) are provided and do not

support the hypothesis that the WMA additives appreciably alter the oxidation kinetics of the base binder. The confidence intervals of *M* values are also provided in Table 12, and similar to the E_{ac} results, the suggestion that *M* values are altered is not supported.

Table 12. Statistical analysis of the optimization.

Asphalt Binder	**Goodness of fit**			**95 % Confidence Interval**	
	SSE	R^2	RMSE	E_{ac} *(kJ/mol)*	*M (a.u.)*
Base	0.08592	0.9488	0.06249	8	0.1302
Emulsion additive	0.10640	0.9429	0.06953	17	0.2451
Zeolite additive	0.06782	0.9399	0.05823	27	0.2291
Chemical additive	0.06295	0.9551	0.05756	9	0.0680

Note: Goodness of fit and E_{ac}/M confidence intervals are provided by multiple non-linear regressions in MATLAB curve fitting tool. SSE: Sum of squares due to error; R^2: The coefficient of multiple determination; Adjusted R^2: Adjusted R^2based on the residual degrees of freedom; RMSE: Root mean squared error.

Correlations between kinetics parameters

The kinetics data for the base binder and for the WMA modified binders of this study are consistent with previously reported correlations for E_{ac}, E_{af}, A_c and A_f [21]. Figure 25(a) shows the empirical correlation between the fast-rate activation energy (E_{af}) and the constant-rate activation energy (E_{ac}) for the results of both this work and previous research. The WMA modified asphalts follow the same trend; this correlation could be used to estimate the fast rate reaction parameters from the constant rate parameters. Figure 25(b) shows the correlation of the constant-rate activation energy (E_{ac}) to the pre-exponential factor (A_c). The exponential correlation is clear, with R^2 above 0.99. The correlation between E_{ac} and A_c indicates an isokinetic temperature (T_{iso}),

at which all asphalt binders age at the same rate. Figure 25(c) shows the correlation between fast-rate reaction parameters E_{af} and A_f.

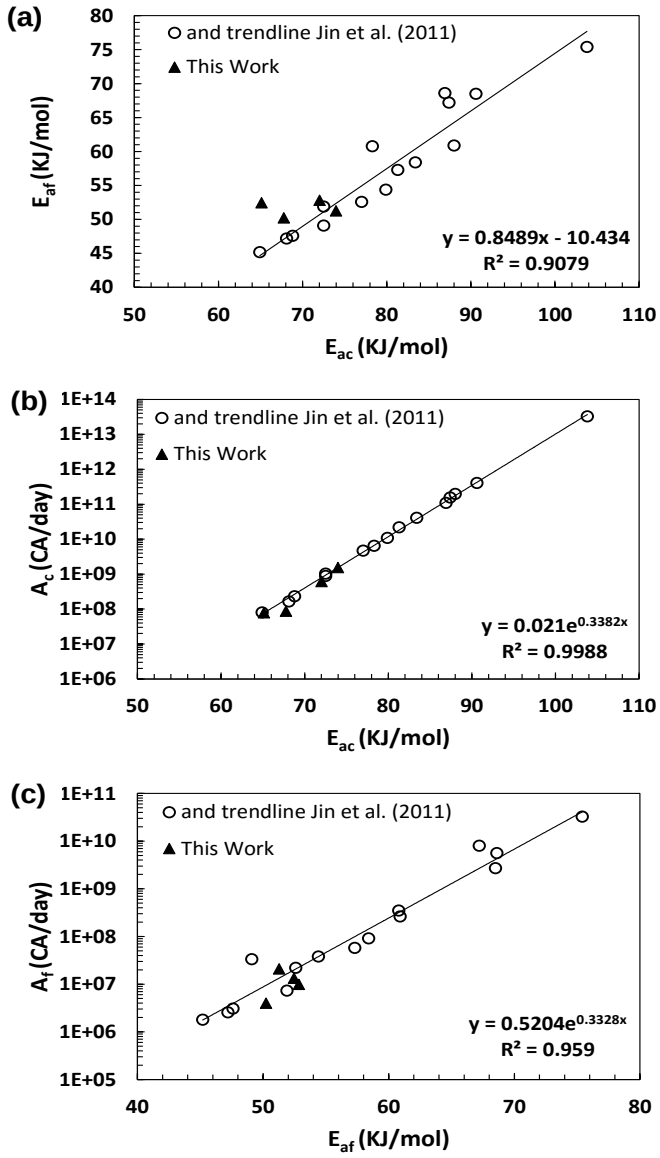

Figure 25. Kinetics parameters of Table 11 compared to the correlations of previous research: (a) empirical linear correlation between the fast rate and constant rate activation energies; (b) isokinetic temperature correlation for the constant-rate reaction; (c) Correlation between fast-rate kinetics parameters.

Pavement aging simulation

Asphalt oxidation kinetics data can be used in a pavement binder oxidation model to predict binder oxidation and hardening in service [30]. The governing equation of this model is shown below:

$$\frac{\partial P(x,t)}{\partial t} = \frac{\partial y}{\partial x}\left(fcf \cdot D_0 \frac{\partial P}{\partial x}\right) - \frac{c}{h} \cdot \frac{\partial CA(x,t)}{\partial t} \quad (19)$$

Principle concepts of this model are briefly explained. *P* means the partial pressure of oxygen in the asphalt; *t* refers to time and *x* means the distance to air void/asphalt interface; *c* is the factor convert *CA* formation rate to oxygen consumption rate and *h* is the solubility constant of oxygen in asphalt. A field calibration factor (*fcf*) is introduced to adjust D_0. The initial condition of this model is zero oxygen concentration in asphalt; the boundary conditions are partial pressure equals 0.2 at the air void/asphalt interface and $\frac{\partial P(x,t)}{\partial x}\Big|_{x=D_d} = 0$.

As an example comparison, a 10-year pavement aging simulation was performed with E_{ac} values selected to represent the high and low values of the WMA materials reported in Table 11 plus the high value previously reported in the literature for hot mix asphalt materials (105 kJ/mol) and a mid-range value (85 kJ/mol); A_c, E_{af} and A_f values were calculated based on the literature correlations shown in Figure 25. Other simulation inputs were assumed to be the same for all binders, including: pavement depth (12.7 mm), diffusion depth (1 mm), starting viscosity (1000 Pa s), a viscosity hardening susceptibility (*HS*) (3.16/CA), field calibration factor (*fcf*) (1), *M* value (0.2016 a.u.), CA_{tank} value (0.559 a.u.) and climate data (hourly solar radiation and air temperature,

daily average wind speed) for Lubbock, TX. Other model parameters are shown in the figure (*fcf* is the field calibration factor and may be used to take into account changes in oxygen transport to the binder due, e.g., to the development of microcracks).

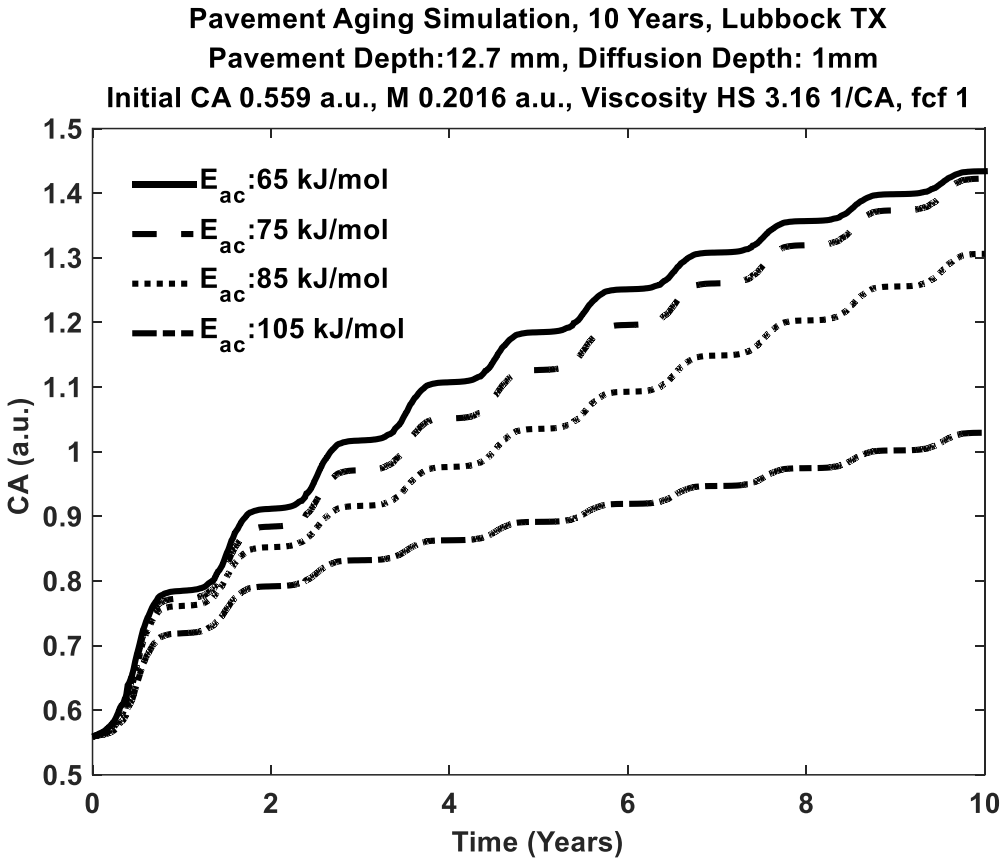

Figure 26. Example pavement aging simulation showing the effect of different E_{ac} values with other parameters selected according to the correlations shown in Figure 25.

A few general observations can be made based on the simulations shown in Figure 26. First, a lower activation energy results in a higher reaction rate, and vice versa. Thus, the material with E_{ac}= 65 kJ/mol has the highest rate (CA increases most quickly over time) while the material with E_{ac} = 105 kJ/mol has the lowest. Second, over

time, 10 years for example, the results vary significantly for the extremes in E_{ac} values. Third, note that the high-activation energy response is essentially linear (after the initial fast-rate period and in terms of average rate over the 10-year period) whereas the low-activation energy has a clearly declining rate, over time. This is a reflection of the effect of the increasingly harder binder (and consequently increasingly lower oxygen diffusion coefficient) as oxidation proceeds and the resulting differences in the balance (or competition) between the oxidation reaction rate and the oxygen diffusion rate (through the binder film that surrounds each air void pore); a constant slope indicates that the CA rate of increase is not limited by oxygen transport, whereas the curve that progresses to a decreasing slope over time reflects the effect of an increasing diffusion resistance as the binder hardens due to oxidation. The balance between reaction and diffusion rates is important; the lower activation energy results in a higher reaction rate (than for the higher activation energy) and thus a higher demand for the diffusion rate to keep up with the reaction and deliver oxygen to the asphalt surrounding the air void pores.

Some specific observations also can be made. The 65 kJ/mol and 75 kJ/mol curves begin to deviate after 1.5 years because of the faster reaction rate at 65 kJ/mol; however, after 8 years, the gap begins to narrow as the 65 kJ/mol rate continues to slow because of the increasing diffusion resistance described above. Considering the WMA range of Eac values estimated in this study (65–75 kJ/mol), and the statistical results in Table 12, there is no support for an hypothesis that there is a statistically significant difference between the asphalt aging kinetics of WMA binders and their corresponding base binder, suggesting that no adverse effect of WMA additives on the asphalt

oxidation kinetics is found. Of note, this pavement aging simulation section is focused on the effect of activation energies, other parameters such as pavement depth, viscosity hardening susceptibility and climate profile are fixed. Thus, this conclusion should not be generalized to all WMA pavements. The 85 kJ/mol and 105 kJ/mol curves, on the other hand, provide a larger context for the effects of the various oxidation rates that might be encountered for different asphalt materials.

Conclusion

To study the oxidation kinetics of warm mix asphalt, aging experiments and subsequent kinetics parameter estimations were conducted in this study. Besides determining the kinetics parameters, statistical analysis on the regression and an example pavement aging simulation were also conducted. The key findings of this work are:

- The fast-rate, constant-rate oxidation reaction model was used to describe oxidation reaction data for WMA materials. The five kinetics parameters for the model (E_{ac}, A_c, E_{af}, A_f, and M) were estimated from a least squares optimization procedure. Statistical analysis of the E_{ac} values (the governing parameter in the asphalt oxidation kinetics model, because of the parameter correlations) shows no significant difference between the base binder and its WMA binders oxidation kinetics.
- WMA asphalt binders follow the same correlations between the four parameters for the k_c and k_f reaction rate constants as previously established for 15 base binders. These correlations provide a practical way of making

reasonable, relatively rapid estimates of kinetics parameters from minimal E_{ac} reaction data for pavement durability design.

- The parameters were used in an example pavement aging simulation to explore possible effects of differences in activation energy on pavement aging, holding all other variables constant. Simulation results suggest that for the activation energy range spanned by the base binder and its corresponding WMA binders (65 to 75 kJ/mol), no significant difference in pavement oxidation would occur over 10 years of pavement service. By comparison, other activation energies (85 and 105 kJ/mol) show significantly less oxidation over the same timeframe. Of note, this pavement aging simulation contains hypothetical parameters and this conclusion should not be generalized for all WMA pavements.
- The simulations also demonstrate the competition for oxygen that can occur between diffusion and reaction and the impact that an increasing diffusion resistance can have by slowing the pavement oxidation rate over the course of the pavement life.

To summarize, the oxidation kinetics of some popular WMA binders were determined. Results show that no significant adversely effect of WMA additives on oxidation kinetics was discovered. An example of the pavement aging simulation containing hypothetical materials covering the WMA kinetics range were given, to address how to use these kinetics parameters to predict pavement aging.

CHAPTER V

CONCLUSIONS AND RECOMMENDATIONS

Fundamental understanding of asphalt chemical and mechanical properties are critical for a satisfactory pavement design and extended pavement durability. In this dissertation, asphalt absorption into porous aggregate and the warm mix asphalt oxidation kinetics are extensively investigated. The key findings of this research are summarized as following:

Conclusion

Asphalt absorption

The conventional method for asphalt absorption measurement requires a subjective saturate surface dry condition. Unsurprisingly, this conventional asphalt absorption procedure suffers a lot from precision issue [38]. To reduce the measurement error, a new method using density gradient column, was developed in this research.

The density gradient column method can directly measure the density of small particles (e.g. aggregate mass between 0.1 – 3 g), providing the capacity to study detailed aggregate characteristics and asphalt absorption. In this research, six types of aggregates were investigated, experimental result showed that although the aggregates characteristics varied from piece to piece. The asphalt absorption correlated very well with the void volume, suggesting that the volume based asphalt absorption to be a universal indicator. Subsequent study on the loose mix materials confirmed this correlation. Additionally, a study on the contacting condition of asphalt absorption

suggested that the mixing/curing time and temperature can affect the final absorption value significantly. An empirical asphalt absorption models was also proposed, to calculate the absorption level over time. Meanwhile, theoretical explanation on the asphalt absorption mechanism was also discussed.

Oxidation kinetics

Warm mix asphalt technology has been widely deployed in the pavements to reduce the cost and extend workability. Although research on the warm mix asphalt rheology can be found elsewhere, the oxidation kinetics of warm mix asphalt has not been reported. In order to study the oxidation kinetics, necessary for the pavement aging prediction, a well-developed POV method was applied to the warm mix asphalt.

The fast-rate constant-rate reaction model was applied to describe oxidation reaction data for warm mix asphalt. Statistical analysis of the E_{ac} values (the governing parameter in the asphalt oxidation kinetics model, because of the parameter correlations) shows no significant difference between the base binder and its warm mix asphalt binders. A pavement simulations covering the kinetics parameters of warm mix asphalt material and conventional materials demonstrate that the competition for oxygen that can occur between diffusion and reaction and the impact that an increasing diffusion resistance can have by slowing the pavement oxidation rate over the course of the pavement life.

Recommendations

The density gradient column has been proved to be an efficient tool to measure asphalt absorption. The experiment of asphalt absorption and contacting time suggests

that the air void is not “saturated” after 15 seconds mixing and 2 hours curing. Moreover, longer mixing time experiments show that the void fraction of absorption binder can be above 80%. These results imply that the absorption process is still under “kinetics control.” Thus, collecting more asphalt absorption data using density gradient column while addressing the surface energy, pore size distribution, contacting time and temperature would be very interesting. Additionally, oxidation kinetics studies on activation energy suggest that there are insignificant difference between warm mix asphalt and their base binder control. These results provide necessary information to improve the pavement durability by optimizing the pavement design. It is helpful to go on extend the understanding of asphalt additives from the oxidation perspective.

The following future work is recommended.

(1) It has been reported that the air void size can affect the asphalt absorption value. As DGC provided the opportunity to study the asphalt absorption in individual aggregate piece, it is suggested to measure aggregate pore size distribution in a certain aggregate piece and compare with its asphalt absorption value. This comparison would provide necessary information to improve and validate asphalt absorption model.

(2) DGC can measure density of small particles directly, thus providing better precision than the saturated surface dry based conventional practice. Besides aggregate density, asphalt density could also be measured. A preliminary experiment on aged asphalt binders showed that the density of asphalt increase with aging. It is possible that as the oxygen react with the asphalt,

the mass of oxygen are combined into the reaction products. Systemically experiments on asphalt density are suggested to study the reason of this increased density and how they would affect the pavement performance.

(3) The DGC method could be incorporated into the pavement design to estimate asphalt absorption. In this research, based on the five types of natural aggregate results, asphalt absorption correlates very well with the air void volume. And, the volumetric fraction of absorbed asphalt tend to be consistent, under same mixing/curing procedure. This information can be used in the pavement design to provide more detailed information for asphalt absorption estimation. Details steps of this estimation are described as following:

   a. Before the construction of pavement, for a specific combination of aggregate/asphalt materials, its corresponding asphalt absorption could be measured using DGC method.
   b. Then, the fraction of air void occupied by absorbed asphalt can be calculated.
   c. Using this fraction, together with the air void volume data (which would be provided in pavement design), the total amount of absorbed binder can be estimated more precisely.
   d. An adjustment of binder content, based on the DGC correlation can then be applied to make up the effective binder loss.

(4) The kinetics study on warm mix asphalt show that there is insignificant difference between warm mix asphalt binder and their based binder control. The concentrations of warm mix additives used in this study are determined from the industrial standards. To further evaluate the effect of warm mix additives, an experiment on more concentrations would be helpful. Also, there is other WMA technology with no additives (e.g. foaming WMA). Its oxidation kinetics should be studied, if possible.

(5) Besides warm mix asphalt technology, the recycled asphalt pavement (RAP) and recycled asphalt shingle (RAS) are also widely used in asphalt industry. To recover the properties of these heavily aged asphalt, recycling agent need to be added. However, it is not clear if the recovered asphalt binder would undergo a similar oxidation path as the neat binder. It is also unknown if the recycling agent would affect the oxidation kinetics. An experiment on the oxidation kinetics of RAP/RAS would be helpful.

(6) Hardening susceptibility of warm mix asphalt could affect the final pavement durability under oxidation stress. It is suggested to study the hardening susceptibility of warm mix asphalt, to better correlate the chemical properties (carbonyl area) to the rheological properties (viscosity and G-R parameter).

(7) A pavement aging simulation was conducted in this study. However, this simulation needs to be validated with field sample of warm mix asphalt. It is suggested to collect the field sample of warm mix asphalt pavements, and to compare the field data to simulation results.

REFERENCES

[1] J. Petersen, P. Harnsberger, Asphalt aging: dual oxidation mechanism and its interrelationships with asphalt composition and oxidative age hardening, Transportation Research Record 1638 (1998) 47-55.

[2] J.W. Button, C. Estakhri, A. Wimsatt, A synthesis of warm mix asphalt, Report FHWA/TX-07/0-5597-1, 2007. Texas Transportation Institute, College Station, TX.

[3] S.D. Capitão, L.G. Picado-Santos, F. Martinho, Pavement engineering materials: Review on the use of warm-mix asphalt, Construction and Building Materials 36 (2012) 1016-1024.

[4] A. Chowdhury, J.W. Button, A review of warm mix asphalt, Report SWUTC/08/473700-00080-1, 2008. Texas Transportation Institute, College Station, TX.

[5] G.C. Hurley, B.D. Prowell, Evaluation of potential processes for use in warm mix asphalt, Journal of the Association of Asphalt Paving Technologists 75 (2006) 41-90.

[6] Ó. Kristjánsdóttir, S. Muench, L. Michael, G. Burke, Assessing potential for warm-mix asphalt technology adoption, Transportation Research Record 2040 (2007) 91-99.

[7] ASTM. C127, Standard Test Method for Specific Gravity and Absorption of Coarse Aggregate, American Society for Testing and Materials, Philadelphia, PA, 1993.

[8] ASTM. C128, Standard Test Method for Specific Gravity and Absorption of Fine Aggregate, American Society for Testing and Materials, Philadelphia, PA, 1993.

[9] F. Hveem, Use of the centrifuge kerosene equivalent as applied to determine the required oil content for dense graded bituminous mixtures, Materials and Research Department, California Division of Highways, 1942.

[10] J. Goshorn, F. Williams, Absorption of Bituminous Materials by Aggregates, Proc. Association of Asphalt Paving Technol 13 (1942) 41-51.

[11] D. Lee, W. Campen, L. Krchma, N. Mcleod, The relationship between physical and chemical properties of aggregates and their asphalt absorption, Proc. Association of Asphalt Paving Technologists. 38 (1969) 242-275.

[12] P.S. Kandhal, D.-Y. Lee, Asphalt absorption as related to pore characteristics of aggregates, Highway Research Record 404 (1972) 97-111.

[13] P.S. Kandhal, M.A. Khatri, Relating asphalt absorption to properties of asphalt cement and aggregate, Transportation Research Record 1342 (1992) 76-76.

[14] P.S. Kandhal, M.A. Khatri, Evaluation of asphalt absorption by mineral aggregates, Report 91-4. 1991. National Center for Asphalt Technology, Auburn, AL.

[15] J.A. Guin, H.-S. Chang, S.-C. Yen, C.-T. Kuo, Absorption of asphalt into porous aggregates: test of a simple physicochemical model, Fuel Science & Technology International 10 (1992) 649-680.

[16] R. Clark, Practical results of asphalt hardening on pavement life, Proc. Association of Asphalt Paving Technologists 27 (1958) 196-208.

[17] P.C. Doyle, Cracking characteristics of asphalt cement, Proc. Association of Asphalt Paving Technologists 27 (1958) 581-597.

[18] P.S. Kandhal, M.E. Wenger, Asphalt properties in relation to pavement performance, Transportation Research Record 544 (1975) 1-13.

[19] P. Kandhal, Low-temperature ductility in relation to pavement performance, ASTM STP 628 C.R. Marek. Ed., American Society of Testing and Materials, 1977. pp 95-106.

[20] P. Kandhal, W. Koehler, Significant studies on asphalt durability: pennsylvania experience (discussion), Transportation Research Record 999 (1984) 41-50.

[21] N.A. Al-Azri, S.H. Jung, K.M. Lunsford, A. Ferry, J.A. Bullin, R.R. Davison, C.J. Glover, Binder oxidative aging in Texas pavements: Hardening rates, hardening susceptibilities, and impact of pavement depth, Transportation Research Record 1962, (2006) 12-20.

[22] C.J. Glover, R.R. Davison, C.H. Domke, Y. Ruan, P. Juristyarini, D.B. Knorr, S.H. Jung, Development of a new method for assessing asphalt binder durability with field validation, Report FHWA/TX-05/1872-2, 2005. Texas Transportation Institute, College Station, TX.

[23] M. Liu, K.M. Lunsford, R.R. Davison, C.J. Glover, J.A. Bullin, The kinetics of carbonyl formation in asphalt, AIChE Journal 42 (1996) 1069-1076.

[24] C.H. Domke, R.R. Davison, C.J. Glover, Effect of oxidation pressure on asphalt hardening susceptibility, Transportation Research Record 1661 (1999) 114-121.

[25] X. Jin, R. Han, Y. Cui, C.J. Glover, Fast-rate–constant-rate oxidation kinetics model for asphalt binders, Industrial & Engineering Chemistry Research 50 (2011) 13373-13379.

[26] Y.H. Huang, Pavement analysis and design, Englewood Cliffs, N.J: Prentice Hall. 1993.

[27] M.S. Buchanan, An evaluation of selected methods for measuring the bulk specific gravity of compacted hot mix asphalt (HMA) mixes, Proc. Association of Asphalt Paving Technologists, 69 (2000) 608-634.

[28] E.R. Brown, P.S. Kandhal, F.L. Roberts, Y.R. Kim, D.-Y. Lee, T.W. Kennedy, Hot mix asphalt materials, mixture design, and construction, NAPA Research and Education Foundation, NAPA Education Foundation, Lanham, Md. 2009.

[29] C.W. Curtis, K. Ensley, J. Epps, Fundamental properties of asphalt-aggregate interactions including adhesion and absorption, Report SHRP-A-341.1993. National Research Council, Strategic Highway Research Program, Washington, DC.

[30] C.W. Curtis, Y.W. Jeon, D.J. Clapp, Adsorption of asphalt functionalities and oxidized asphalts on aggregate surfaces, Fuel Science & Technology International 7 (1989) 1225-1268.

[31] Y. Tan, M. Guo, Using surface free energy method to study the cohesion and adhesion of asphalt mastic, Construction and Building Materials 47 (2013) 254-260.

[32] R. Luo, R.L. Lytton, Selective absorption of asphalt binder by limestone aggregates in asphalt mixtures, Journal of Materials in Civil Engineering 25 (2012) 219-226.

[33] J.D. Doyle, I.L. Howard, Factors affecting the measurement of effective specific gravity for reclaimed asphalt pavement, International Journal of Pavement Research and Technology 5 (2012) 128-131.

[34] J.D. Doyle, I.L. Howard, W.J. Robinson, Prediction of absorbed, inert, and effective bituminous quantities in reclaimed asphalt pavement, Journal of Materials in Civil Engineering 24 (2011) 102-112.

[35] Y. Hou, X. Ji, X. Su, W. Zhang, L. Liu, Laboratory investigations of activated recycled concrete aggregate for asphalt treated base, Construction and Building Materials 65 (2014) 535-542.

[36] A. Pasand ń, I. P érez, Laboratory evaluation of hot-mix asphalt containing construction and demolition waste, Construction and Building Materials 43 (2013) 497-505.

[37] T. Xu, H. Wang, Z. Li, Y. Zhao, Evaluation of permanent deformation of asphalt mixtures using different laboratory performance tests, Construction and Building Materials 53 (2014) 561-567.

[38] ASTM. D4469, Standard practice for calculating percent asphalt absorption by the aggregate in an asphalt pavement mixture, American Society for Testing and Materials Philadelphia, PA, 2011.

[39] J. Haddock, K. Hall, A review of aggregate and asphalt mixture specific gravity measurements and their impacts on asphalt mix design properties and mix acceptance, Report 12-06, 2009. National Center for Asphalt Technology, Auburn, AL.

[40] S. Coombs, A density-gradient column for determining the specific gravity of fish eggs, with particular reference to eggs of the mackerel Scomber scombrus, Marine Biology 63 (1981) 101-106.

[41] J. Fortuin, Theory and application of two supplementary methods of constructing density gradient columns, Journal of Polymer Science 44 (1960) 505-515.

[42] R. Hammonds, C. Stephens, A. Wills, R. Hallman, R. Benson, Behavior of polyethylene in a variable temperature density gradient column, Polymer Testing 32 (2013) 1209-1219.

[43] Texas DOT, Standard specifications for construction and maintenance of highways, streets, and bridges, Item 292, Austin, Texas. 2004, pp. 191-192.

[44] C.J. Glover, G. Liu, A.A. Rose, Y. Tong, F. Gu, M. Ling, E. Arambula, C.K. Estakhri, R.L. Lytton, Evaluation of binder aging and its influence in aging of hot mix asphalt concrete, Report FHWA/TX-14/0-6613-1, 2014. Texas Transportation Institute, College Station, TX.

[45] Y. Ruan, R.R. Davison, C.J. Glover, An investigation of asphalt durability: relationships between ductility and rheological properties for unmodified asphalts, Petroleum Science and Technology 21 (2003) 231-254.

[46] E.I. Ahmed, S.A.M. Hesp, S.K. Paul Samy, S.D. Rubab, G. Warburton, Effect of warm mix additives and dispersants on asphalt rheological, aging, and failure properties, Construction and Building Materials 37 (2012) 493-498.

[47] A. Banerjee, A. de Fortier Smit, J.A. Prozzi, The effect of long-term aging on the rheology of warm mix asphalt binders, Fuel 97 (2012) 603-611.

[48] Q. Qin, M.J. Farrar, A.T. Pauli, J.J. Adams, Morphology, thermal analysis and rheology of Sasobit modified warm mix asphalt binders, Fuel 115 (2014) 416-425.

[49] F. Xiao, V.S. Punith, S.N. Amirkhanian, Effects of non-foaming WMA additives on asphalt binders at high performance temperatures, Fuel 94 (2012) 144-155.

[50] Z.A. Arega, A. Bhasin, T.D. Kesel, Influence of extended aging on the properties of asphalt composites produced using hot and warm mix methods, Construction and Building Materials 44 (2013) 168-174.

[51] F. Farshidi, D. Jones, J.T. Harvey, Warm-mix asphalt study: evaluation of hot and warm mix asphalt with respect to binder aging, Report No. UCPRC-RR-2013-02. 2013. University of California, Pavement Research Center, Davis, CA

[52] A. Jamshidi, M.O. Hamzah, Z. You, Performance of warm mix asphalt containing Sasobit®: state-of-the-art, Construction and Building Materials 38 (2013) 530-553.

[53] S.-J. Lee, S.N. Amirkhanian, N.-W. Park, K.W. Kim, Characterization of warm mix asphalt binders containing artificially long-term aged binders, Construction and Building Materials 23 (2009) 2371-2379.

[54] F. Safaei, J.S. Lee, L.A.H. Nascimento, C. Hintz, Y.R. Kim, Implications of warm-mix asphalt on long-term oxidative ageing and fatigue performance of asphalt binders and mixtures, Road Materials and Pavement Design 15 (2014) 45-61.

[55] C.H. Domke, R.R. Davison, C.J. Glover, Effect of oxygen pressure on asphalt oxidation kinetics, Industrial & Engineering Chemistry Research 39 (2000) 592-598.

[56] R. Han, X. Jin, C.J. Glover, Modeling pavement temperature for use in binder oxidation models and pavement performance prediction, Journal of Materials in Civil Engineering 23 (2011) 351-359.

[57] N. Prapaitrakul, R. Han, X. Jin, C.J. Glover, A transport model of asphalt binder oxidation in pavements, Road Materials and Pavement Design 10 (2009) 95-113.

[58] R. Grover Allen, D.N. Little, A. Bhasin, C.J. Glover, The effects of chemical composition on asphalt microstructure and their association to pavement performance, International Journal of Pavement Engineering 15 (2014) 9-22.

[59] J.C. Petersen, A review of the fundamentals of asphalt oxidation: chemical, physicochemical, physical property, and durability relationships, Transportation Research E-Circular 140, 2009. Transportation Research Board, Washington, DC.

[60] Y. Ruan, R.R. Davison, C.J. Glover, The effect of long-term oxidation on the rheological properties of polymer modified asphalts, Fuel 82 (2003) 1763-1773.

[61] M. Liu, M.A. Ferry, R.R. Davison, C.J. Glover, J.A. Bullin, Oxygen uptake as correlated to carbonyl growth in aged asphalts and asphalt Corbett fractions, Industrial and Engineering Chemistry Research 37 (1998) 4669-4674.

[62] M. Sugano, J. Kajita, M. Ochiai, N. Takagi, S. Iwai, K. Hirano, Mechanisms for chemical reactivity of two kinds of polymer modified asphalts during thermal degradation, Chemical Engineering Journal 176–177 (2011) 231-236.

[63] G. King, M. Anderson, D. Hanson, P. Blankenship, Using black space diagrams to predict age-induced cracking, 7th RILEM International Conference on Cracking in Pavements, Springer, Netherlands. 2012, pp. 453-463.

[64] X. Jin, Y. Cui, C.J. Glover, Modeling asphalt oxidation in pavement with field validation, Petroleum Science and Technology 31 (2013) 1398-1405.

[65] K. Martin, R. Davison, C. Glover, J. Bullin, Asphalt aging in Texas roads and test sections, Transportation Research Record 1269 (1990) 9-19.

[66] C.K. Lau, Reaction rates and hardening susceptibilities as determined from POV aging of asphalts, Transportation Research Record 1342 (1992) 50-57.

APPENDIX

AMRL statistics on water absorption

AASHTO Materials Reference Laboratory (AMRL) has a large database, including compilations of statistics water absorption and aggregate apparent and bulk densities for both coarse and fine aggregates. The single operator and multilaboratory precision for both coarse and fine aggregate absorption can be find from AMRL online database.

For these AMRL data, the level of multilaboratory precision for fine aggregate water absorption, expressed as the difference two-sigma limit in percent (d2s%), ranges from 50 to 141 percent and for coarse aggregate water absorption, the range is from 21 to 108 percent. The single operator d2s% precision values range from 24 to 60 percent for fine aggregate, and for coarse aggregate the range is from eight to 53 percent. These are all quite large values for water absorption uncertainty and should be noted by practitioners. Asphalt absorption precision would be expected to have worse precision than these water absorption numbers.

Furthermore, the large decrease in precision from single operator to multilaboratory (60 percent maximum d2s% compared to over 100 percent maximum) likely can be largely attributed to the subjectivity of operator judgment, specifically concerning the saturated surface dry condition. This conjecture is consistence with the literature report on water absorption.

An evaluation on the precision of conventional method for asphalt absorption

ASTM D4469 is a standard practice that provides a calculation procedure for asphalt absorption. However, detailed statistical measures of precision are not provided. The purpose of this section is to provide estimation on asphalt absorption precision to allow an improved understanding of the reliability of the conventional method.

In order to further evaluate combined asphalt absorption measurement uncertainties, an error propagation function is used to estimate the error in standard methods. Assuming interactions between independent variables are negligible, a common formula for calculating error propagation is the variance formula

$$s_f = \sqrt{\left(\frac{\partial f}{\partial x}\right)^2 {s_x}^2 + \left(\frac{\partial f}{\partial y}\right)^2 {s_y}^2 + \left(\frac{\partial f}{\partial z}\right)^2 {s_z}^2 + \cdots} \quad (20)$$

where s_f represents the standard deviation of error in measuring the function *f(x, y, z,...)* that results from random errors in the independent variables *x, y, z,…*, variables that are characterized by standard deviations s_x, s_y, s_z, … It is important to note that this formula is based on the linear characteristics of the gradient of f and therefore is a good estimation for the standard deviation of *f* as long as s_x, s_y, s_z… are small compared to the partial derivatives.

As an example, we present calculated estimates of the statistical 1s values for water absorption and compare them to the reported AMRL corresponding values that derived from the hundreds of laboratory measurements. Then, we present a corresponding calculation for asphalt absorption, for which there are no laboratory 1s values available.

In AMRL data, water absorption can be represented as:

$$\text{Water absorption (mass percent)} \equiv \frac{\text{mass of absorbed water}}{\text{mass of aggregate}} \text{ x } 100$$

$$= \frac{\text{volume of absorbed water}}{\text{mass of aggregate}} \text{ x water density x } 100$$

$$= \frac{100}{\text{bulk specific gravity of aggregate}} - \frac{100}{\text{apparent specific gravity of aggregate}}$$

From the reported precision for bulk specific gravity and apparent specific gravity of sample 165, we can perform an error propagation calculation for water absorption, presented in Table 13.

Table 13. Error propagation on water absorption, based on AMRL coarse aggregate sample 165, multilaboratory.

	Aggregate Bulk Specific Gravity	**Aggregate Apparent Specific Gravity**
Value	2.713	2.735
s	0.0063	0.0048
$\frac{\partial f}{\partial x}$	-0.136	0.134
$\left(\frac{\partial f}{\partial x}\right)^2 s_x{}^2$	7.34×10^{-7}	4.14×10^{-7}

Based on the calculation, the multilaboratory 1s for water absorption is estimated to be 0.107 mass percent whereas from the water absorption AMRL database, it is 0.063 mass percent. So, the estimated error of water absorption on AMRL coarse aggregate sample #165 is in reasonable agreement to the experimental determination provided in the AMRL database. From this example, we can see error propagation function does provided meaningful information.

Now, recall the equation for calculating asphalt absorption in ASTM D4469:

$$A_{ac} = 100\left[\frac{P_{tac}}{100-P_{tac}} + \frac{G_{ac}}{G_{ag}} - \frac{100G_{ac}}{(100-P_{tac})G_{tm}}\right] \quad (21)$$

where:

A_{ac} = absorbed asphalt as percent by mass of the oven-dry aggregate.

P_{tac} = asphalt content as percent by mass of the total mix in the sample of oven- dry paving mixture.

G_{ac} = apparent specific gravity of the asphalt in the paving mixture sample.

G_{ag} = weighted average ASTM oven-dry bulk specific gravity of the total aggregate in the sample of paving mixture.

G_{tm} = theoretical maximum specific gravity of the sample of oven-dry paving mixture.

Taking the example calculation in ASTM D4469 as an example and referring to ASTM D2041, D6307, D3289 and C127, four variables in the example calculations of ASTM D4469 come into play and their values and distribution statistics are listed in Table 14. The single lab and multiple lab standard deviations were obtained from the other ASTM methods referenced by D4469.

Table 14. Error of variables related to ASTM D4469.

Variables in D4469	Value	Standard Deviation single lab*	Standard Deviation multiple lab*
Asphalt Content weight percent of mix	6.2000	0.04 %	0.06 %
Asphalt Specific Gravity	1.0150	0.0006	0.0007
Bulk Specific Gravity of aggregate	2.6730	0.0090	0.0250
Theoretical Maximum Specific Gravity	2.5010	0.0080	0.0160

Table 15 lists calculated estimates of asphalt absorption errors for the example given in ASTM D4469 based on the error propagation function and values of P_{tac}, G_{ac}, G_{ag} and G_{tm} for the sample calculation in ASTM D4469; standard deviations for the four variables were obtained from the standard methods ASTM D2041, D6307, D3289 and C127.

Table 15. Error propagation calculation on asphalt absorption, ASTM D4469

		P_{tac}	G_{ac}	G_{ag}	G_{tm}
Value	Single Lab	6.2000	1.0150	2.6730	2.5010
	Mutiple Lab	6.2000	1.0150	2.6730	2.5010
s	Single Lab	0.0400	0.0006	0.0090	0.0080
	Mutiple Lab	0.0600	0.0007	0.0250	0.0160
$\frac{\partial f}{\partial x}$	Single Lab	0.6753	-5.2157	-14.2059	17.2996
	Mutiple Lab	0.6753	-5.2157	-14.2059	17.2996
$\left(\frac{\partial f}{\partial x}\right)^2 {s_x}^2$	Single Lab	0.0007	0.0000	0.0163	0.0192
	Mutiple Lab	0.0016	0.0000	0.1261	0.0766

Based on these data and using the error propagation function, the estimated statistical information for asphalt absorption in the example in D4469 calculation is estimated in Table 16.

Table 16. Estimated error statistics for binder absorption in ASTM D4469

	Asphalt Absorption	**Calculated Error Propagation Estimates**			
		1s	**d2s**	**1s%**	**d2s%**
Single lab	1.30	0.19	0.54	15	41
Multiple lab	1.30	0.45	1.28	35	98

Note: *d2s*, difference two-sigma limit; *1s*, one sigma standard deviation.

Confidence interval of water absorption and asphalt absorption

In statistics, confidence interval is used to describe how reliable a measurement is. Practically, 95 % confidence interval are most widely used. From the standard deviation data, plus the replicates of sample, a confidence interval on the reputed number could be estimated. In this study, the 95 % confidence interval of water absorption and asphalt absorption are calculated. An example of the 95 % confidence interval is provided below (as an example, the water absorption is 30.4 by weight percent, and standard deviation is 2.5 by weight percent):

Table 17. Confidence interval calculation of the water absorption

n	**Standard deviation**	**95% confidence interval**	**Coefficient of variance (c.i.)**
3	0.025	0.062	20.4%
4	0.025	0.040	13.1%
5	0.025	0.031	10.2%
6	0.025	0.026	8.6%
7	0.025	0.023	7.6%
8	0.025	0.021	6.9%
9	0.025	0.019	6.3%
10	0.025	0.018	5.9%

Table 17 indicated that, for single operator when there are only 3 replicates, the 95 % confidence interval of water absorption would be 0.062 by weight of weight percent. This is relatively noticeable (20.4 %) to the water absorption value. It should be noted that the standard deviation of this sample is within the typical range in the AMRL

database. A further calculation indicated that when the replicates need to reach 5, to maintain the 95 % confidence interval at 10 %.

A similar calculation on asphalt absorption is also provided. From the single operator one standard deviation data calculated from Table 16 (as an example, the asphalt absorption is 1.3 by weight percent, whereas the standard deviation to be 0.19 by weight percent).

Table 18. Confidence interval calculation of the asphalt absorption

n	**Standard deviation**	**95% confidence interval**	**Coefficient of variance (c.i.)**
3	0.0019	0.005	36.3%
4	0.0019	0.003	23.3%
5	0.0019	0.002	18.1%
6	0.0019	0.002	15.3%
7	0.0019	0.002	13.5%
8	0.0019	0.002	12.2%
9	0.0019	0.001	11.2%
10	0.0019	0.001	10.5%

Table 18 shows the 95% confidence interval of asphalt absorption, based on the error propagation calculation. At same replicates level, the asphalt absorption has less precision than the water absorption (e.g. when n=3, 36.3%). Moreover, if 10 % coefficient of variance is preferred, at least ten replicates is necessary for asphalt absorption measurement.

Comparing the water absorption between DGC and AMRL

The water absorption precision of DGC and AMRL data are calculated and compared in the following table:

Table 19. Comparing the water absorption precision: DGC and AMRL

Method	Sample	Value	1s	d2s	COV (1s)	COV (d2s)
DGC Water absorption (g)	Delta Sandstone 1	0.034	0.005	0.015	0.153	0.432
	Delta Sandstone 6	0.298	0.009	0.026	0.031	0.087
AMRL water absorption (mass percent)	Sample 165	0.304	0.063	0.178	0.207	0.586
	Sample 166	0.294	0.061	0.173	0.207	0.587
	Sample 167	0.574	0.135	0.382	0.235	0.665
	Sample 168	0.591	0.142	0.402	0.240	0.680

Note: *d2s*, difference two-sigma limit; *1s*, one sigma standard deviation.

Table 19 shows the comparison of water absorption from DGC method and conventional method. The conventional method data are from AMRL database. DGC water absorption precision is sensitive to the sample. Two aggregate particles of Delta Sandstone show different confidence level. However, despite the variance of DGC water absorption precision, it is relatively less than the conventional practice.